Title

Fokker–Planck linearization for non-Gaussian stochastic elastoplastic finite elements

Authors

Karapiperis, Konstantinos
Sett, Kallol
Kavvas, M Levent
et al.

Publication Date

2016-08-01

DOI

10.1016/j.cma.2016.05.001

Peer reviewed

Fokker–Planck linearization for non-Gaussian stochastic elastoplastic finite elements

Author links open overlay panelKonstantinosKarapiperis[a]KallolSett[b]M.Levent Kavvas[a]BorisJeremić[ac]
Show more

https://doi.org/10.1016/j.cma.2016.05.001Get rights and content

Highlights

- Stochastic elastoplastic boundary value problems are addressed in a polynomial chaos-based spectral stochastic finite element framework.
- A nonlocal Fokker–Planck–Kolmogorov equation is employed at the constitutive level.
- A linearization procedure is developed merging the constitutive to the finite element level.
- Different constitutive models are investigated.

Abstract

Presented here is a finite element framework for the solution of stochastic elastoplastic boundary value problems with non-Gaussian parametric uncertainty. The framework relies upon a stochastic Galerkin formulation, where the stiffness random field is decomposed using a multidimensional polynomial chaos expansion. At the constitutive level, a Fokker–Planck–Kolmogorov (FPK) plasticity framework is utilized, under the assumption of small strain kinematics. A linearization procedure is developed that serves to update the polynomial chaos coefficients of the expanded random stiffness in the elastoplastic regime, leading to a nonlinear least-squares optimization problem. The proposed framework is illustrated in a static shear beam example of elastic-perfectly plastic as well as isotropic hardening material.

- **Previous** article
- **Next** article

Keywords

Fokker–Planck equation
Elastoplasticity
Stochastic finite elements
Linearization
Polynomial chaos
Non-Gaussian

1. Introduction

In constitutive modeling, material parameters are traditionally defined in a deterministic fashion by usually extracting the mean from a number of experiments. However, the behavior of all engineering materials, let alone geomaterials, is inherently uncertain, as portrayed by various researchers [1], [2], [3]. The uncertain response follows from inherent uncertainty of material behavior and/or spatial non-uniformity of material distribution. In addition, the nonlinear material behavior present in several engineering applications is usually described using elastoplastic constitutive relations. The physical or phenomenological components of such a model are ideally described by random fields, most of which are non-Gaussian. Modeling them as Gaussian fields can induce both inaccuracy and instability to the solution of a boundary value problem. For example, a Gaussian representation of the material stiffness results in inaccurate higher order moments while physically allowing negative realizations of the process to occur (softening). To realistically approximate such a physical quantity, a strictly positive definite field is required.

Intrusive uncertainty quantification (UQ) frameworks, in which the uncertainty is propagated through the governing differential equations, are in many cases more efficient than non-intrusive ones. However, most researchers have focused on non-intrusive methods, which are easier to develop and utilize existing computational tools, or have limited their attention to intrusive UQ for simpler problems. The simplest example of a non-intrusive method is Monte Carlo Simulation (MCS) [4], [5], which may be seen as a direct integration method in which the integration points are chosen randomly over the probability space. Depending on the application, the latter approach can prove so computationally demanding that any practical application is hindered, at least for elasto-plastic models. Lately, more sophisticated sampling-based approaches have been developed including stochastic collocation [6], [7] and non-intrusive Galerkin techniques [8], [9]. The applicability of those methods is not affected by the complexity

of the problem since they act as wrappers on a deterministic solver which in turn acts as a “black box”.

Several researchers have dealt so far with intrusive uncertainty quantification in computational mechanics with an emphasis on linear problems. A comprehensive review of such methods may be found in [5], [10], [11], where the authors also provide insight to the well-posedness and structure of a stochastic boundary value problem. So far, the most widely used method for the quantification of uncertainty has been the stochastic finite element method (SFEM) [12], which relies on a spectral decomposition of parametric uncertainties and a polynomial chaos [13] approximation of the output random field. It is one of the first developments of a stochastic Galerkin method, where the problem is formulated in a variational form and holds in a weak sense. This class of methods allows for an explicit functional representation of the solution in terms of independent random variables. An overview of stochastic Galerkin methods may be found in [14], [11], [15]. A significant contribution to the efficiency of the above methods with respect to different classes of non-Gaussian processes has been the introduction of the generalized polynomial chaos expansion (gPCE) [16], guaranteeing optimal (exponential) convergence rates through an appropriate choice of orthogonal polynomials from the Askey family. Researchers also have attempted to address the curse of dimensionality associated with these methods by developing sparse approximations through low-rank tensor product techniques [17], proper generalized decompositions and separated representations [18].

The first attempt to extend SFEM to nonlinear material behavior was by Anders and Hori [19], who used a perturbation expansion at the stochastic mean behavior. In computing the mean behavior they took advantage of bounding media approximation by introducing two fictitious bounding bodies providing an upper and a lower bound for the mean. This method, however, inherits the “closure problem” (essentially the need for higher order statistical moments in order to calculate lower order statistical moments) and suffers from the “small coefficient of variation” requirement for the material parameters. Later, Jeremić et al. [20] derived a second-order exact expression for the evolution of the probability density function of stress for elastoplastic constitutive rate equations with uncertain material parameters. Utilizing an Eulerian–Lagrangian form of the Fokker–Planck–Kolmogorov (FPK) equation [21], the aforementioned “closure problem” associated with regular perturbation methods is resolved. Afterwards, Jeremić and Sett [22]modified their approach to account for probabilistic rather than expected yielding and incorporated their developed FPK-based elastoplastic model in a Gaussian spectral stochastic finite element framework [23]. Later, Rosić [24]and Arnst and

Ghanem [25] presented in detail the variational theory behind the mixed-hardening stochastic plasticity problem along with stochastic versions of relevant established computational plasticity algorithms.

In this paper, we utilize an FPK plasticity framework at the constitutive level and a stochastic Galerkin framework at the finite element level. Non-Gaussian parametric uncertainty is considered through a combined Karhunen–Loève/polynomial chaos (KL/PC) expansion. The above are coupled through an FPK linearization scheme that updates the coefficients of the polynomial chaos (PC) approximation of the random stiffness. As opposed to the stochastic extension of classic variational inequality algorithms [24], [25], the FPK equation provides a way to transform the problem to a deterministic advection–diffusion equation and takes advantage of efficient algorithms developed for relevant problems. In addition, it helps overcome potential challenges associated with the accurate approximation of random inequality constrains, present in variational inequality methods (representation of convex elastic cones). Further, this method may be tailored to provide varying order of accuracy counterbalanced by computational efficiency through appropriate selection of the KL/PC spaces in which the constitutive integration procedure is performed. First, the stochastic approximation schemes are discussed followed by the finite element formulation. Next, the underlying FPK framework is introduced along with the proposed linearization procedure and the complete framework is illustrated with a simple static shear beam example.

2. Stochastic discretization

2.1. Elastic stiffness

Any arbitrary non-stationary stiffness random field may be approximated using a combined Karhunen–Loève/polynomial chaos methodology. This technique involves representation of an arbitrary stochastic process as a polynomial of a suitable underlying Gaussian field, whose covariance structure is decomposed by means of the Karhunen–Loève expansion (KLE). Following Sakamoto and Ghanem [26], we represent the uncertain elastic constitutive tensor field with the help of the polynomial chaos expansion (PCE):

(1)

where is a set of Hermite polynomials of an underlying Gaussian set and is an element of the space of random variables . The variable denotes the order of the PCE. It can be shown that the latter is convergent in ; a relevant convergence rate study can be found in [27].

The spatially dependent coefficients may be computed via simple projection but this kind of expansion is defined without any reference to the random field and the expected accuracy is low. Therefore, a correlation structure is endowed to the underlying field by considering the following multidimensional PC representation:

(2)

where is now a set of multidimensional Hermite polynomials of an underlying correlated Gaussian field . The orthogonality of the polynomials is employed to calculate the coefficients as:

(3)

where the numerator can be evaluated with the inverse CDF approach using some type of numerical quadrature (e.g., collocation, Monte Carlo (MC), quasi Monte Carlo (QMC), etc.). The correlation function of induced on is given as the solution to the following polynomial equation [26]:

(4)

where denote two spatial points in the domain of interest. This equation is solved by discretizing the domain into a number of nodes and solving the resulting system of equations with the following constraint:

(5)

Knowing the above, the correlated random field may be expanded in the following Karhunen–Loève form:

(6)

subject to the following constraint deriving from the unit variance condition imposed on :

(7)

In the above equations, and denote the resulting eigenvalues and eigenvectors respectively, and denotes the dimensionality of the truncated expansion. It is required that we re-normalize to a unit variance as follows:

(8)

By equating the two representations of in Eqs. (1), (2), we can find the coefficients as

(9)

where is the order of the polynomial and is an index on at least one of the making up . Note that the accuracy of the synthesized marginal probability density function depends mainly on the order of the PC expansion, while the correlation accuracy depends on the dimension of . In the case of arbitrary non-Gaussian processes, the suitability of KLE as a means of characterizing the random variables entering the PCE or gPCE [16] is questionable. This is because, in this case, KLE yields uncorrelated but dependent random variables. Adaptation of the general PC framework to suitably

chosen probability measures is presented in [28]. Often, in this case, transformation techniques such as the Rosenblatt [29] or the Nataf [30]transform are utilized.
This study assumes a strictly positive definite lognormal random stiffness field in conjunction with classical PCE [31], which admits the analytical computation of the respective coefficient (rather than the numerical techniques described above). Assuming an underlying Gaussian field , the actual stiffness field is given by:
(10)
with the following mean and variance relations:
(11)
(12)
The process is expanded in the Karhunen–Loève sense as:
(13)
and projection into polynomial chaos yields analytical coefficients :
(14)
Fig. 1 shows how the synthesized marginal probability density function using this methodology converges to the target lognormal distribution for a case of COV=30% for an increasing order of polynomial chaos approximation. Fig. 2, on the other hand, compares the target and approximated correlation structure for varying KL dimensionality.

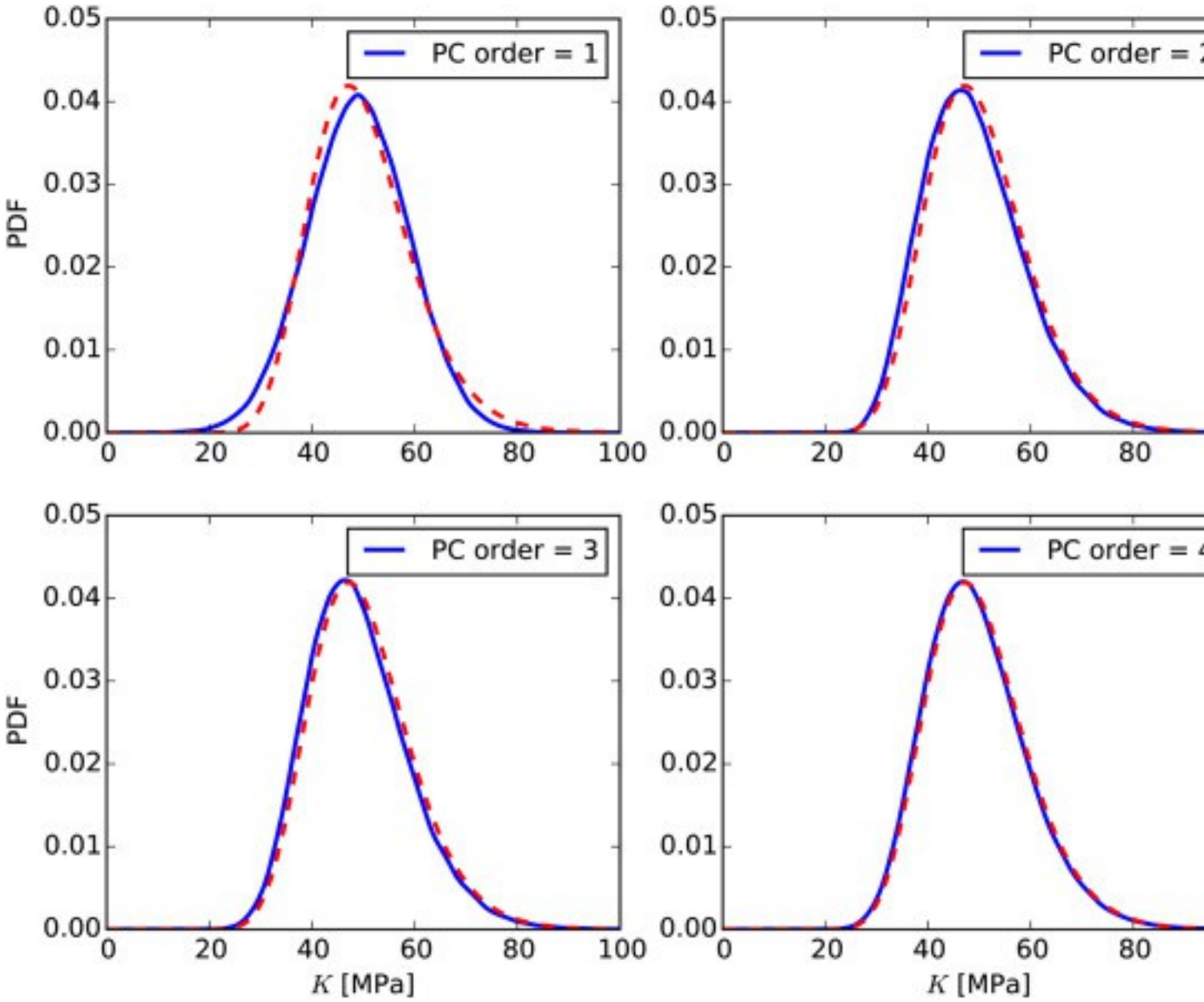

1. Download full-size image

Fig. 1. Convergence of the PC approximation (blue) to the target (red) lognormal distribution. (For interpretation of the references to color in this figure legend, the reader is referred to the web version of this article.)

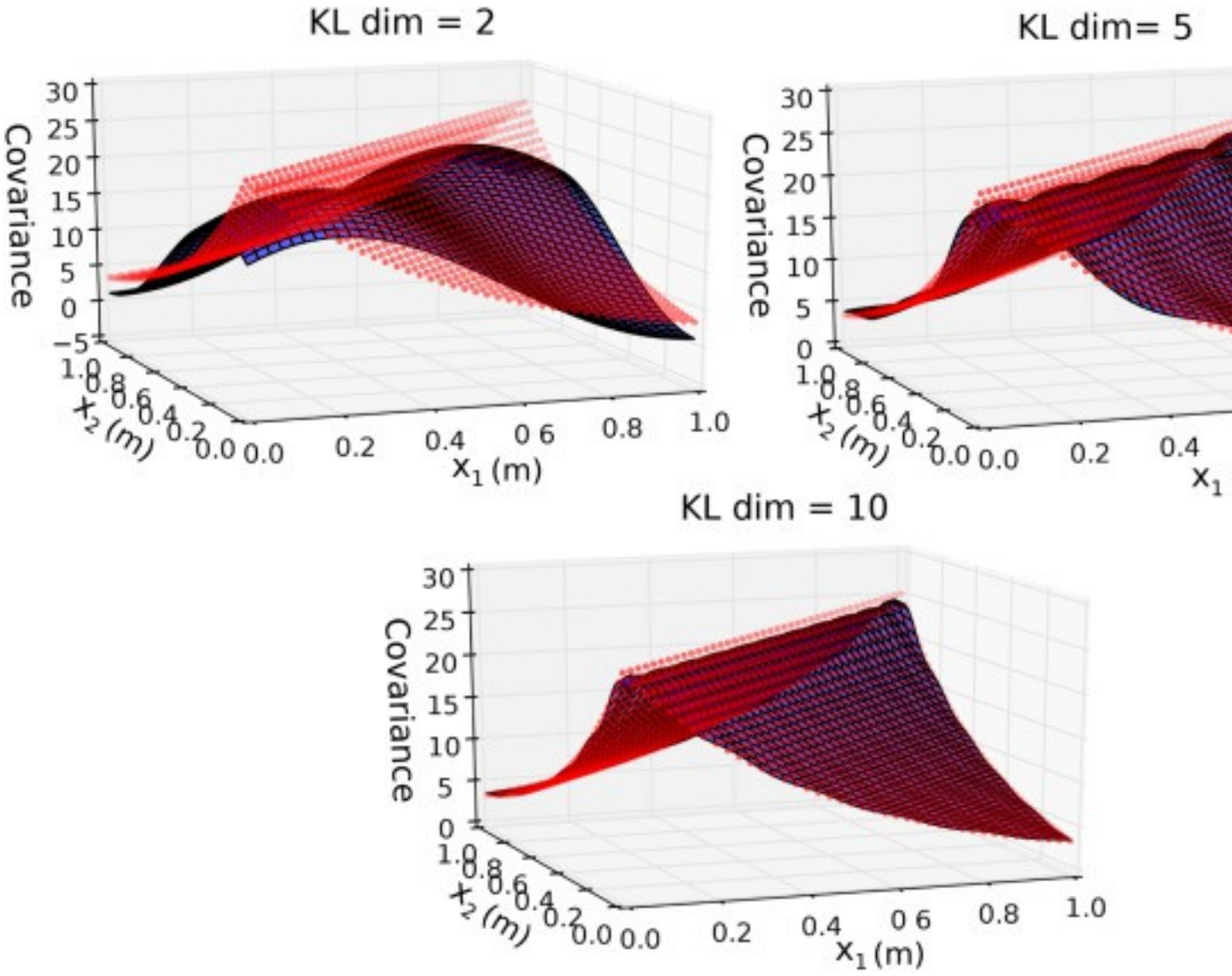

1. Download full-size image

Fig. 2. Comparisons of the approximated (blue) and the target (red) correlation structures for varying KL dimensionality. (For interpretation of the references to color in this figure legend, the reader is referred to the web version of this article.)

2.2. Shear strength

In the case of a non-Gaussian shear strength random field , the above methodology may be applied considering the two fields to be independent of each other. Alternatively, for computational efficiency, one may go with a Gaussian random field. In this case, however, care should be taken so that the shear strength remains bounded and positive in order to ensure physical behavior and well-posedness of the problem [32]. Note that

this choice may impose a tight restriction on the applicable coefficient of variation. Then, the shear strength field may be approximated simply by a KLE as follows:
(15)
by considering the following Fredholm integral equation of the second kind [33] with the covariance function as a kernel:
(16)∫DCSu(x1,x2)fk(x1)dx1=λkfk(x2).
This expansion is optimal in the sense that it is the best approximation that may be achieved in the L2(D)⊗L2(Ω) norm.
In some cases (e.g., triangular, exponential kernel) the above eigenproblem may be solved analytically, but in the general case a numerical approximation scheme is required. In that sense, a number of methods have been applied including FEM [12], wavelet-Galerkin [34], H-matrices [35] and meshless methods [36].
In a standard finite element setting, each eigenfunction, fk of the kernel is approximated as:
(17)fk(x)=∑i=1Ndikhi(x)
where h and d represent basis functions of compact support and appropriate nodal coefficients, respectively. Utilizing the above representation and requiring the error to be orthogonal to the approximating space, one may transform Eq. (16) to the following weak form:
(18)∑i=1Ndik[∫D∫DCSu(x1,x2)hi(x2)hj(x1)dx1dx2−λk∫Dhi(x)hj(x)dx]=0.
The required discretization (mesh size) depends on the correlation length describing the rate of fluctuation of the random field. It has been shown [37], [38] that 2–4 elements per correlation length are usually enough to capture the structure of the random field. For example, a 1-dimensional 10 m long domain requires a 20–40 element mesh for lc=1m, while only 2–4 elements are adequate for lc=10m. In cases where the correlation structure is approximated by long-tailed kernels (e.g., Gaussian), the resulting generalized “stiffness” matrix in the eigenproblem looses its sparsity resulting in an inefficient numerical solution. It is therefore common to modify (truncate) the kernels so as to increase the sparsity of the representation. Melink and Korelc [39]studied this problem in terms of numerical integration and loss of positive definiteness of the covariance matrix.

3. Spatial and stochastic discretization of the solution

The unknown displacement random field is semi-discretized in the stochastic dimension using PCE:
(19)u(x,θ)=∑i=0Pdi(x)Ψi[ξr(θ)]

where $\Psi_i[\xi_r(\theta)]$ represents a set of random Hermite polynomials of order P. The component $d_i(x)$ is, then, further discretized in the spatial sense using standard finite element shape functions:

$$d_i(x)=\sum_{j=1}^{N} d_{ij} N_j(x). \tag{20}$$

This results in a final expression for the random displacement field:

$$u(x,\theta)=\sum_{i=0}^{P}\sum_{j=1}^{N} d_{ij} N_j(x)\Psi_i[\xi_r(\theta)]. \tag{21}$$

4. Finite element formulation

Employing the Galerkin weak formulation of linearized static FEM [40], we have the following simplified form :

$$\sum_e \left[\int_{D_e} \nabla N_m(x) D(x,\theta) \nabla N_n(x) dV u - \int_{D_e} f_m(x,\theta) dV\right]=0 \tag{22}$$

where $\sum_e$ denotes the assembly procedure over all finite elements of the discretized domain V and $f_m(x)$ incorporates the various elemental contributions to the global force vector.

Combining Eqs. (1), (21), (22) and denoting the shape function gradients as:

$$\nabla N_n(x) := B_n(x) \tag{23}$$

yields:

$$\sum_e \left[\int_{D_e} B_m(x) \sum_{i=0}^{M} r_i(x)\Phi_i[\{\xi_r(\theta)\}] B_n(x) \sum_{j=0}^{P} d_{nj}\Psi_j[\xi_r(\theta)] dV - \int_{D_e} f_m(x,\theta) dV\right]=0. \tag{24}$$

Taking now the Galerkin projection of the discretized equation onto each arbitrary polynomial basis of the displacement approximation $\Psi_k[\xi_r(\theta)]$:

$$\sum_e \left[\int_{D_e} B_m(x) \sum_{i=0}^{M} r_i(x)\Phi_i[\{\xi_r(\theta)\}] B_n(x) \sum_{j=0}^{P}\sum_{k=0}^{P} d_{nj}\Psi_j[\xi_r(\theta)]\Psi_k[\xi_r(\theta)] dV - \int_{D_e}\sum_{k=0}^{P} f_m(x,\theta)\Psi_k[\xi_r(\theta)] dV\right]=0. \tag{25}$$

Taking expectation on both sides results in the following system of equations:

$$\sum_{n=1}^{N}\sum_{j=0}^{P} d_{nj}\sum_{k=1}^{M} b_{ijk} K_{mni} = F_m \langle \Psi_k[\{\xi_r\}] \rangle \tag{26}$$

where

$$K_{mni}=\int_D B_m(x) r_i(x) B_n(x) dV \tag{27}$$

and

$$F_m=\int_D f_m(x,\theta) dV. \tag{28}$$

Symbolic manipulations are carried out using Mathematica [41] in order to precompute the coefficients of the tensor:

$$b_{ijk}=\langle \Phi_i[\{\xi_r\}]\Psi_j[\{\xi_r\}]\Psi_k[\{\xi_r\}] \rangle. \tag{29}$$

The form of the latter induces a special block sparsity in the resulting stiffness matrix that may be exploited to develop an efficient solution scheme. Several researchers have dealt with such systems of equations arising in the context of the spectral stochastic finite element formulation. One of the first attempts was made by Ghanem and Kruger [42] who proposed two solution procedures, a preconditioned CG method as

well as a hierarchical formulation. Another iterative scheme of the family of Krylov-subspace methods that has been applied is the preconditioned MINRES [43]. In addition, researchers have developed multi-grid approaches [44] as well as incomplete block-diagonal preconditioning schemes based on the FETI-PD solver [45]. A more complete review of the methods may be found in [24].

5. Elastoplasticity

In this study, the elastoplastic behavior is treated in a spectral fashion by updating the coefficients of the stochastic approximation of the stiffness according to an underlying Fokker–Planck–Kolmogorov framework. At each integration point and orthogonal multidimensional PC space, the nonlinear FPK equation is solved incrementally, and an optimization procedure yields the equivalent linearized advection and diffusion terms. The updated PC coefficients are then computed based on these terms. We investigate varying approximation accuracy by restricting the number of spaces in which the integration procedure is carried out.

5.1. Formulation of FPK-based probabilistic elastoplasticity

The incremental form of spatial-average elastoplastic constitutive equation may be written as

(30)$$d\sigma_{ij}(x_t,t)dt=D_{ijkl}(x_t,t)d\epsilon_{kl}(x_t,t)dt$$

where $D_{ijkl}(x_t,t)$ is the continuum stiffness tensor, evaluated at the spatial coordinate x_t, and can be either elastic or elasto-plastic:

(31)$$D_{ijkl}=\{D_{ijkl}^{el};f<0\vee(f=0\wedge df<0)D_{ijkl}^{el}-D_{ijmn}^{el}\frac{\partial U}{\partial\sigma_{mn}}\frac{\partial f}{\partial\sigma_{pq}}D_{pqkl}^{el}\frac{\partial f}{\partial\sigma_{rs}}D_{rstu}^{el}\frac{\partial U}{\partial\sigma_{tu}}-\frac{\partial f}{\partial q^*}r^*;f=0\wedge df<0$$

according to the established Karush–Kuhn–Tucker conditions.

In the above equation, D_{ijkl}^{el} is the elastic stiffness tensor, f is the yield function, which is a function of stress σ_{ij} and internal variables q^* (scalar, vector- or tensor-valued), while U is the plastic potential function. In its most general form, the incremental constitutive equation takes the form

(32)$$d\sigma_{ij}(x_t,t)dt=\beta_{ijkl}(\sigma_{ij},D_{ijkl},q^*,r^*;x_t,t)d\epsilon_{kl}(x_t,t)dt$$

or

(33)$$d\sigma_{ij}(x_t,t)dt=\eta_{ijkl}(\sigma_{ij},D_{ijkl},\epsilon_{kl}(x_t,t)q^*,r^*;x_t,t)$$

where the stochasticity of the operator β is induced by the stochasticity of D_{ijkl},q^*,r^*. This renders the above equation a linear/non-linear ordinary differential equation with stochastic coefficients. Similarly randomness in the forcing term (ϵ_{kl}) results in a linear/non-linear ordinary differential equation with stochastic forcing. Combining the two

cases yields a linear/non-linear ordinary differential equation with stochastic coefficients and stochastic forcing. Using the Eulerian–Lagrangian form of the FPE equation [21] the above equation takes the following form in the probability density space

(34)$$\partial P(\sigma ij,t)\partial t=-\partial\partial\sigma mn[\{\square\eta mn(\sigma mn(t),Dmnrs,\epsilon rs(t))\square +\int 0tdt\tau Cov0[\partial\eta mn(\sigma mn(t),Dmnrs,\epsilon rs(t))\partial\sigma ab;\eta ab(\sigma ab(t-\tau),Dabcd,\epsilon cd(t-\tau))]\}P(\sigma ij(t),t)] +\partial 2\partial\sigma mn\partial\sigma ab[\int 0tdt\tau Cov0[\eta mn(\sigma mn(t),Dmnrs,\epsilon rs(t));\eta ab(\sigma ab(t-\tau),Dabcd,\epsilon cd(t-\tau))]P(\sigma ij(t),t)]$$

where $P(\sigma ij,t)$ is the probability density of stress, $\square\cdot\square$ is the expectation operator, $Cov0[\cdot]$ is the time-ordered covariance operator and ηij is a generalized random tensor operator. Details of this derivation can be found in [20]. The above equation is equivalent to the following generalized form:

(35)$$\partial P(\sigma ij,t)\partial t=-\partial\partial\sigma mn[N(1)mn\sigma eqP(\sigma ij,t)-\partial\partial\sigma ab\{N(2)mnab\sigma eqP(\sigma ij,t)\}]$$

where $N(1)$ and $N(2)$ are advection and diffusion coefficients respectively that are particular to the constitutive model. Given the initial and boundary conditions as well as the second-order statistics of material properties, Eq. (35) may be solved with second-order accuracy.

To account for the uncertainty in the probabilistic yielding, Jeremić and Sett [22] introduced the following equivalent advection and diffusion coefficients:

(36)$$N(1)mn\sigma eq(\sigma ij)=(1-P[f>0])N(1)mnel+P[f>0]N(1)mnep$$

(37)$$N(2)mnab\sigma eq(\sigma ij)=(1-P[f>0])N(2)mnabel+P[f>0]N(2)mnabep$$

where $(1-P[f>0])$ represents the probability of the material being elastic, while $P[f>0]$ represents the probability of the material being elastoplastic. $P[f>0]$ is obtained from the cumulative density function, rendering it an explicit function of the stress σij as well as the internal variables $q*$.

Utilizing Eq. (34), one may compute the elastic and elastoplastic coefficients addressed in Eq. (35) as:

(38)$$N(1)mnel=\square Dmnrsel\dot{\epsilon}rs\square$$

(39)$$N(2)mnabel=tCov0[Dmnrsel\dot{\epsilon}rs;Dabcdel\dot{\epsilon}cd]$$

and

(40)$$N(1)mnep=\square Dmnrsep\dot{\epsilon}rs\square+\int 0tdt\tau Cov0[\partial\partial\sigma ab\{Dmnrsep\dot{\epsilon}rs\};Dabcdep\dot{\epsilon}cd]$$

(41)$$N(2)mnabep=\int 0tdt\tau Cov0[Dmnrsep(t)\dot{\epsilon}rs;Dabcdep(t-\tau)\dot{\epsilon}cd].$$

The evolution of any internal variable qi of the model is handled through a coupled FPK equation of the form:

(42)$$\partial P(qi,t)\partial t=-\partial\partial qm[N(1)mqeq(\sigma mn,qm)P(qi,t)-\partial\partial qn\{N(2)mnqeq(\sigma mn,qm)P(qi,t)\}].$$

The advection and diffusion coefficients in the above equation are given similar to Eqs. (36), (36) but with no contributions of any “elastic” state:

(43)$N(1)mqeq(\sigma ij,qi)=P[f>0]N(1)mqep$

(44)$N(2)mnqeq(\sigma ij,qi)=P[f>0]N(2)mnqep.$

The elastoplastic components of the equivalent advection and diffusion terms are functions of the so-called loading index or plastic multiplier L and the rates of evolution of the internal variables ri:

(45)$N(1)mqep=\square Lri\square+\int 0tdt\tau Cov0[\partial\partial qjLri(t);Lrj(t-\tau)]$

(46)$N(2)mnqep=\int 0tdt\tau Cov0[Lri(t);Lrj(t-\tau)]$

where L may be expressed as:

(47)$L=\partial f\partial\sigma otDijotel\epsilon ij\partial U\partial\sigma abDabcdel\partial f\partial\sigma cd-\partial f\partial qmrm.$

5.2. Linearization for stiffness update

The constitutive integration of the FPK-based plasticity model cannot directly provide the updated generalized stiffness at the finite element level. Therefore, a numerical scheme is required in order to compute the stiffness in a PC expansion form as per Eq. (1). In this study we assume an equivalent linear FPK equation involving the updated PC coefficients which are deduced through a least-squares optimization procedure.

For each orthogonal PC space, s, Eq. (35) applies with the advection and diffusion coefficients taking the form:

(48)$N(1)mnseq(\sigma ijs,x)=(1-P[f>0])N(1)mnel+P[f>0]N(1)mnep$

(49)$N(2)mnabseq(\sigma ijs,x)=(1-P[f>0])N(2)mnabel+P[f>0]N(2)mnabep.$

For the purposes of this study, let us consider an isotropic linear elastic—Mises isotropic hardening model and derive the equivalent advection and diffusion coefficients for this case. The isotropic linear elasticity tensor in Eq. (31) reads:

(50)$Dijklel=G\delta ik\delta jl+(K-23G)\delta ij\delta kl$

where K and G denote the bulk and shear modulus respectively and are represented as random fields (see for example Eq. (1)).

The elastoplastic continuum tangent tensor in Eq. (31) is given in the following general form:

(51)$Dijklep=G\delta ik\delta jl+(K-23G)\delta ij\delta kl-AijAkl*B+KP.$

The Mises linear hardening yield function is written as:

(52)$f=J2-Su=12sijsij-Su.$

Under the assumption of associated flow rule we have:

(53)$\partial f\partial\sigma ij=\partial U\partial\sigma ij$

which results in the following symmetry:

(54)Aij=Aij∗=Dijklel∂f∂σkl.

After some algebraic manipulations, one can easily derive:

(55)Aij=GJ2sijB=G.

The plastic modulus KP is computed here on the basis of a deterministic hardening rule in terms of the equivalent plastic strain:

(56)Su=Su(ϵeqp).

After imposing the consistency condition, we have:

(57)KP=−∂f∂Suk̄=−13∂f∂SudSudϵeqp∂f∂J2=13dSudϵeqp.

Combining Eqs. (36)–(41), (50)–(51), we can derive the final coefficients of the FPK constitutive rate equation as:

(58)N(1)mnseq=(1−P[f>0])□[Gδmrδns+(K−23G)δmnδrs]ϵ̇rs(t)□+P[f>0]□[Gδmrδns+(K−23G)δmnδrs−1G+13dSudϵeqp(GJ2)2sijs(t)skls(t)]ϵ̇rs(t)□+∫0tdτCov0[∂∂σabs{[Gδmrδns+(K−23G)δmnδrs−1G+13dSudϵeqp(GJ2)2sijs(t)skls(t)]ϵ̇rs(t)};[Gδacδbd+(K−23G)δabδcd−1G+13dSudϵeqp(GJ2)2sabs(t−τ)scds(t−τ)]ϵ̇cd(t−τ)]

(59)N(2)mnabseq=(1−P[f>0])tCov0[{Gδmrδns+(K−23G)δmnδrs−1G+13dSudϵeqp(GJ2)2sijs(t)skls(t)}ϵ̇rs(t);[Gδacδbd+(K−23G)δabδcd−1G+13dSudϵeqp(GJ2)2sabs(t)scds(t)]ϵ̇cd(t)]+P[f>0]∫0tdτCov0[{Gδmrδns+(K−23G)δmnδrs−1G+13dSudϵeqp(GJ2)2sijs(t)skls(t)}ϵ̇rs(t);{Gδacδbd+(K−23G)δabδcd−1G+13dSudϵeqp(GJ2)2sabs(t−τ)scds(t−τ)}ϵ̇cd(t−τ)].

The solution of Eq. (35) may only provide the rate of change of the probability density at the kth-step, yet not the updated stiffness at the finite element level. To deduce the latter, let us consider a linearized FPK equation for the stress corresponding to the orthogonal space s at the same computational step in the following form:

(60)∂Plin(σijs,t)∂t=−N(1)mnslin∂P(σijs,t)∂σmns+N(2)mnabslin∂2P(σijs,t)∂σmnsσabs

where the linearized advection and diffusion coefficients are given by:

(61)N(1)mnslin=rmnabs(k)∑i=0P□ΦiΨs□12Δt∑j=1N[Nj,b(x)Δdijak−1+Nj,a(x)Δdijbk−1]

(62)N(2)mnabslin=t(rmnabs(k))2∑i=0PVar[ΦiΨs]14Δt2[Nj,b(x)Δdijak−1+Nj,a(x)Δdijbk−1]2.

In an explicit scheme, the strain increment at the (k−1)th step is utilized, while the fourth-order tensor valued PC coefficient rmnabs(k) is unknown. Depending on the specific constitutive model, the above equations may be simplified to include scalar PC coefficients and deterministic bases in an appropriate tensor format. Combining

Eqs. (35), (60), one ends up with an over-determined residual system of equations in terms of the unknown coefficients at time step k:

(63)Ri(rmnabs(k))=∂Plin(σis,t)∂t−∂P(σis,t)∂t=0,i=1,…,N.

Each equation corresponds to a single point in the stress domain and the system of equations may be solved in the least squares sense using, for example, the Levenberg–Marquardt algorithm [46]. Therefore, a stiffness update procedure is established. A summary of the constitutive update algorithm is given in Algorithm 1.

Algorithm 1 General constitutive update at an integration point

for each PC space **do**
  Compute elastic advection and diffusion coeffs $N^{s^{el}}_{(1)_{mn}}$, $N^{s^{el}}_{(2)_{mnab}}$
  Solve the (trial) elastic stress FPK equation
  Check yield condition
  if $P[f > 0] < TOL$ **then**
    Update stress σ^s_{ij}
  else
    Compute el-pl advection and diffusion coeffs $N^{s^{eq}}_{(1)_{mn}}$, $N^{s^{eq}}_{(2)_{mnab}}$
    Solve elastoplastic stress FPK equation
    Compute int. variable advection and diffusion coeffs $N^{q^{ep}}_{(1)_m}$, $N^{q^{ep}}_{(2)_{mn}}$
    Solve internal variable FPK equation
    Solve linearization problem
    Update stress σ^s_{ij} and internal variables q^s_i
    Update PCE coefficients r^s_{mnab}
  end if
end for

1. Download full-size image

5.3. Varying order of accuracy

The outlined linearization scheme is accurate to the order of the PC approximation of the stiffness. However, one can restrict the accuracy of the method to second order with significant computational time savings, by considering the integration of a single FPK equation at any point in the discretized domain. This is achieved by considering the total stress, σ rather than each PC stress component, σs. The linearized equation becomes:

(64)∂Plin(σij,t)∂t=−N(1)lin∂P(σij,t)∂σmn+N(2)lin∂2P(σij,t)∂σmnσab

where:

(65)N(1)lin=∑s=0Mrmnabs(k)∑i=0P□ΦiΨs□12Δt∑j=1N[Nj,b(x)Δdijak−1+Nj,a(x)Δdijbk−1]
(66)N(2)lin(rsk,x)=t∑s=0M(rmnabs(k))2∑i=0PVar[ΦiΨs]14Δt2[Nj,b(x)Δdijak−1+Nj,a(x)Δdijbk−1]2.

Again, the resulting system of equations is generally over-determined and may be solved for rmnabs(k) using least-squares techniques. Due to the form of the FPK constitutive integrator, we do not expect higher order accuracy in the linearized tangent stiffness. Indeed, the Gaussian nature of this second-order exact variation of the linearization procedure, suggests that the advection and diffusion coefficients at each integration point may be fully described by two independent coefficients (rmnabs(k),s=1,2). This implies that the polynomial chaos coefficients that correspond to third and higher order (rmnabs(k),s≥3) will be dependent (negatively correlated) variables. It is proposed that the higher order coefficients retain their elastic (initial) values in order to achieve higher order accuracy during elastic loading or unloading.

In a more general sense, in order to achieve higher than second order accuracy and at the same time save on computation compared to the procedure proposed in Section 5.2, the integration procedure may be applied to a restricted number of orthogonal PC spaces. The set of spaces in which the integration procedure is eventually carried out may be chosen on the basis of *a posteriori* error estimation techniques. However, a study of the accuracy of such a framework is out of the scope of this study.

6. Numerical illustrations

In this last section, the proposed framework is applied to the static loading of a shear beam representing a one-dimensional soil column under undrained conditions. The idealized numerical model is shown in Fig. 3. Two different cases are considered to test the methodology against parameters that differentiate the contribution of each orthogonal space, the evolution of the stress PDF as well as the global response (Table 1).

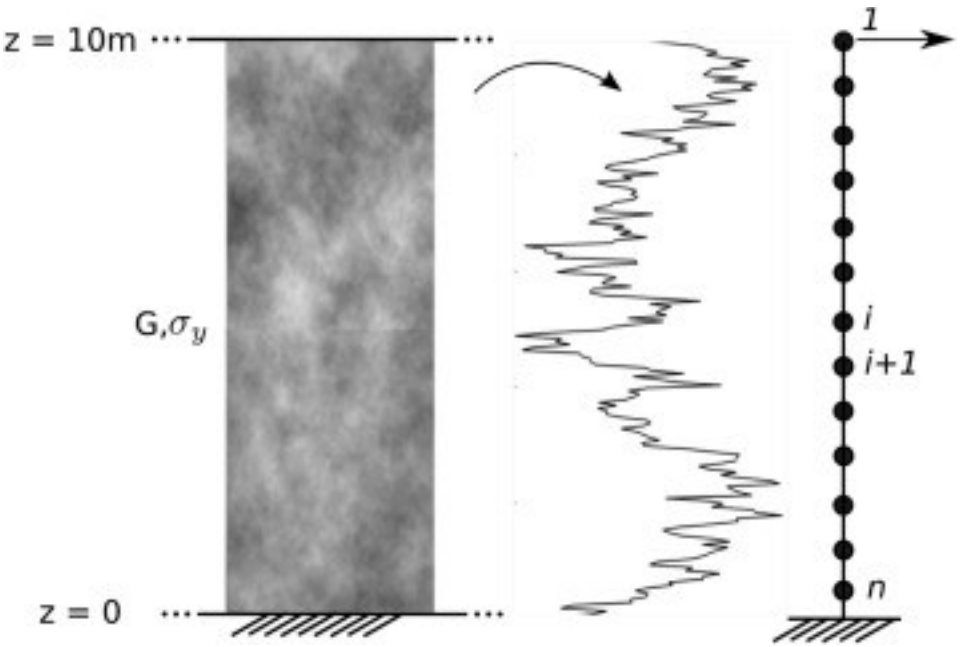

1. Download full-size image

Fig. 3. A realization of the stiffness random field and the idealized numerical model.

Table 1. Parameters for the examples in this study.

Case	lcG,σy (m)	□G□ (MPa)	COVG	□σy□ (MPa)	COVσy
1	0.2	50	0.4	0.8	0.1
2	1	50	0.1	0.8	0.4
Case	KP (MPa)	nKL	mPCd	sPCk	
1	0	2	2	2	
2	20	2	2	2	

Fig. 4 shows the evolution of the PDF of stress at the first 4 orthogonal PC spaces at the top of the shear beam for Case 1. Due to the small correlation length and large coefficient of variation of the shear modulus, all stress spaces are active. The evolution of the PDF in the mean shear stress space is initially diffusive and then sharpens in a quick transition to the elastoplastic regime. On the other hand, the remaining stress spaces exhibit mostly diffusion. The total reconstructed mean and standard deviation of stress versus the mean strain, considering all PC terms, is plotted in Fig. 5, where the transition to the plastic regime is only evident towards the end of the simulation. At the same spatial point, Fig. 6 shows the evolution of PC coefficients derived by means of the proposed linearization procedure. After a few steps, the optimization procedure has converged and the values of the coefficients remain almost constant for the elastic part of the response. Then, the 0th PC space exhibits a sharp decline towards zero, consistent with the mean stress response in an elastic-perfectly plastic body. The rest of

the spaces decline at a smaller rate, in agreement with the evolution of second order stress statistics in those spaces towards the end of loading (see Fig. 4). The evolution of the profile of coefficients (along the depth of the shear beam) is given in Fig. 7, where the shape of the initial profile (light color) is determined by the underlying KL eigenvectors, while the accuracy is governed by the associated truncation error. It is evident that the aforementioned profile values ultimately tend to zero due to the elastic-perfectly plastic nature of the model. Finally, the global force versus (mean ± standard deviation) displacement response at the top is shown in Fig. 8, where we can identify a sharp transition to a perfectly plastic response.

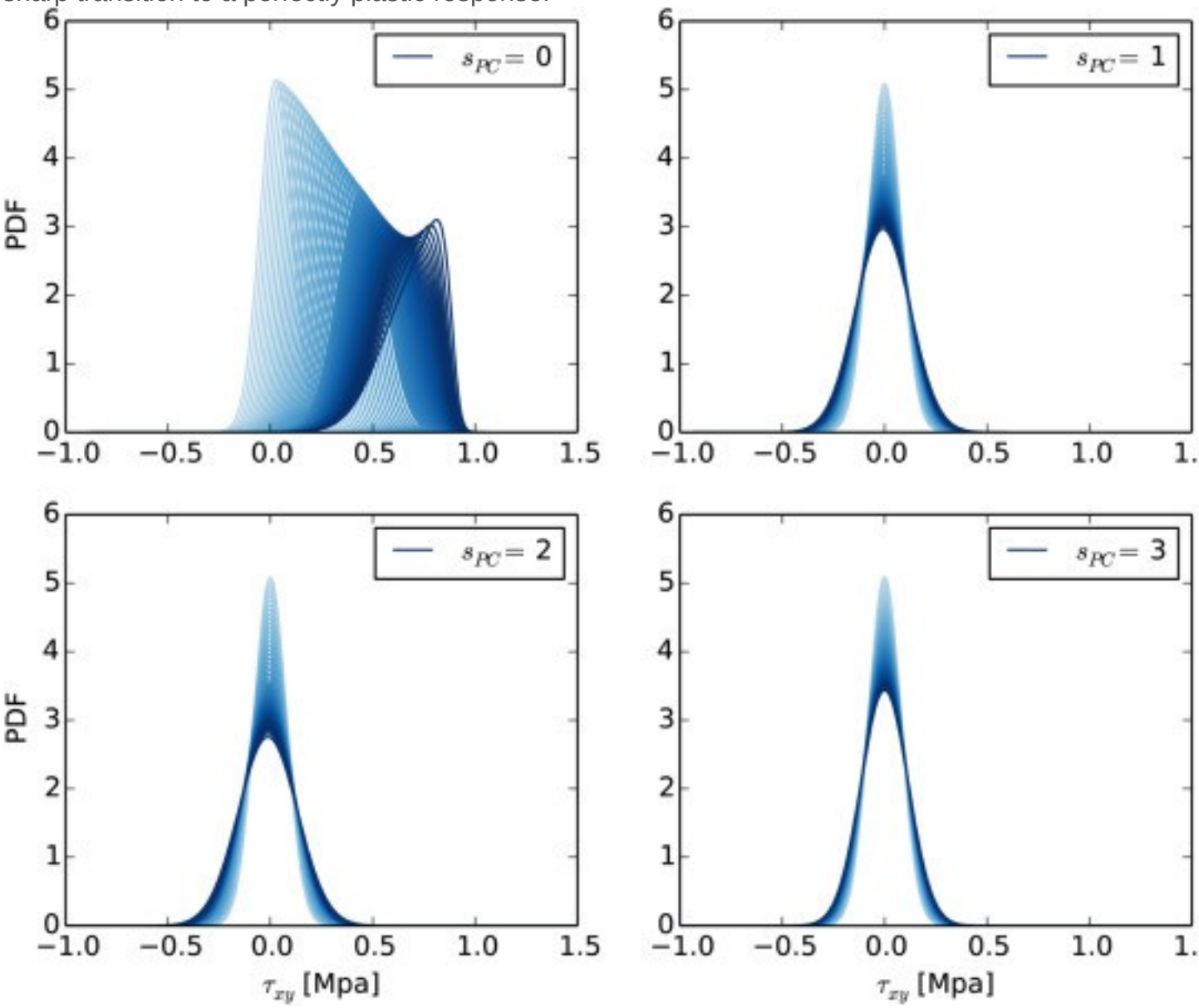

1. Download full-size image

Fig. 4. Evolution of the PDF of shear stress at the first 4 orthogonal PC spaces (Case 1).

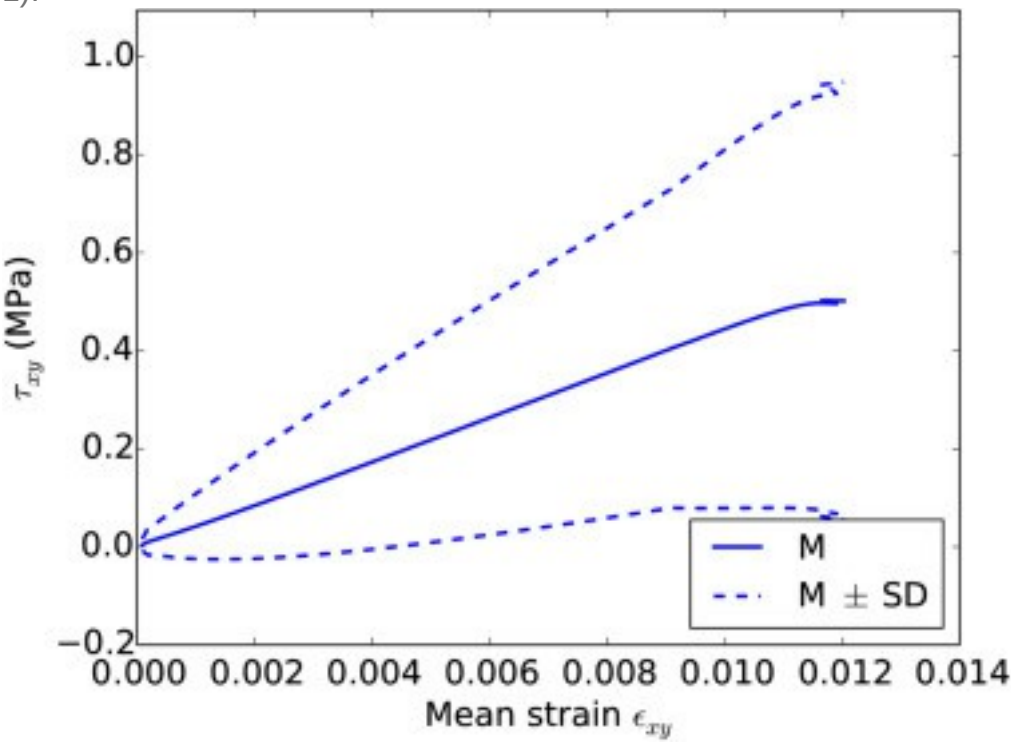

1. Download full-size image

Fig. 5. Mean (M) ± standard deviation (SD) of stress versus mean strain response at the top of the shear column (Case 1).

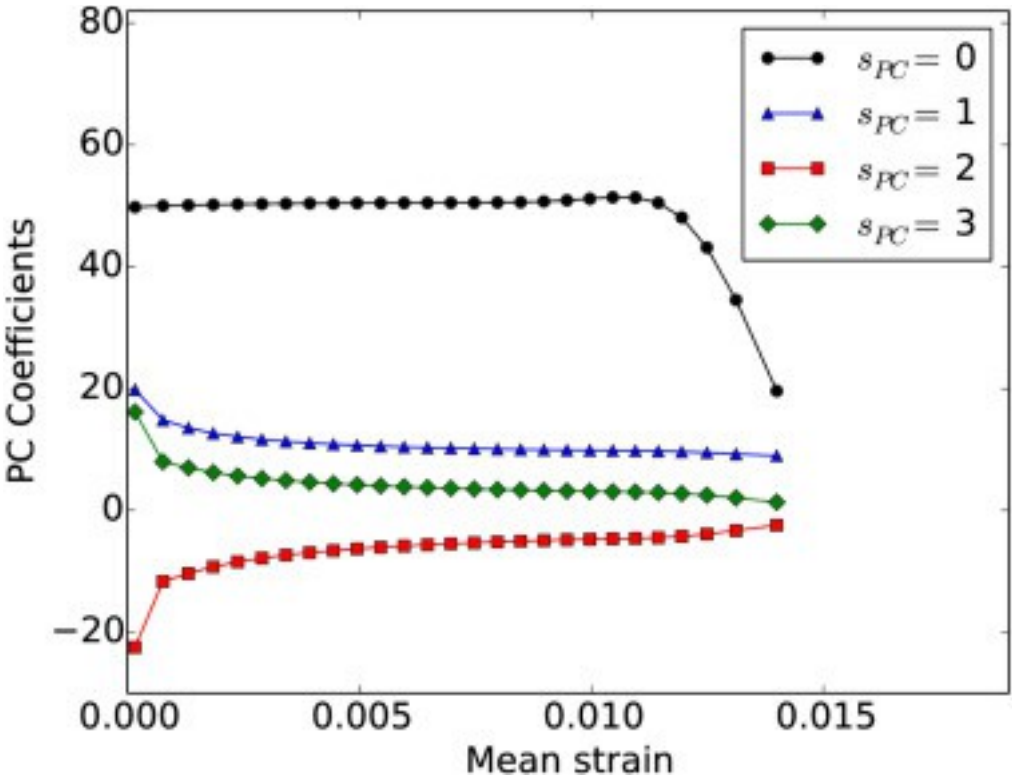

1. Download full-size image

Fig. 6. Evolution of PC coefficients of the linearized random shear stiffness (Case 1).

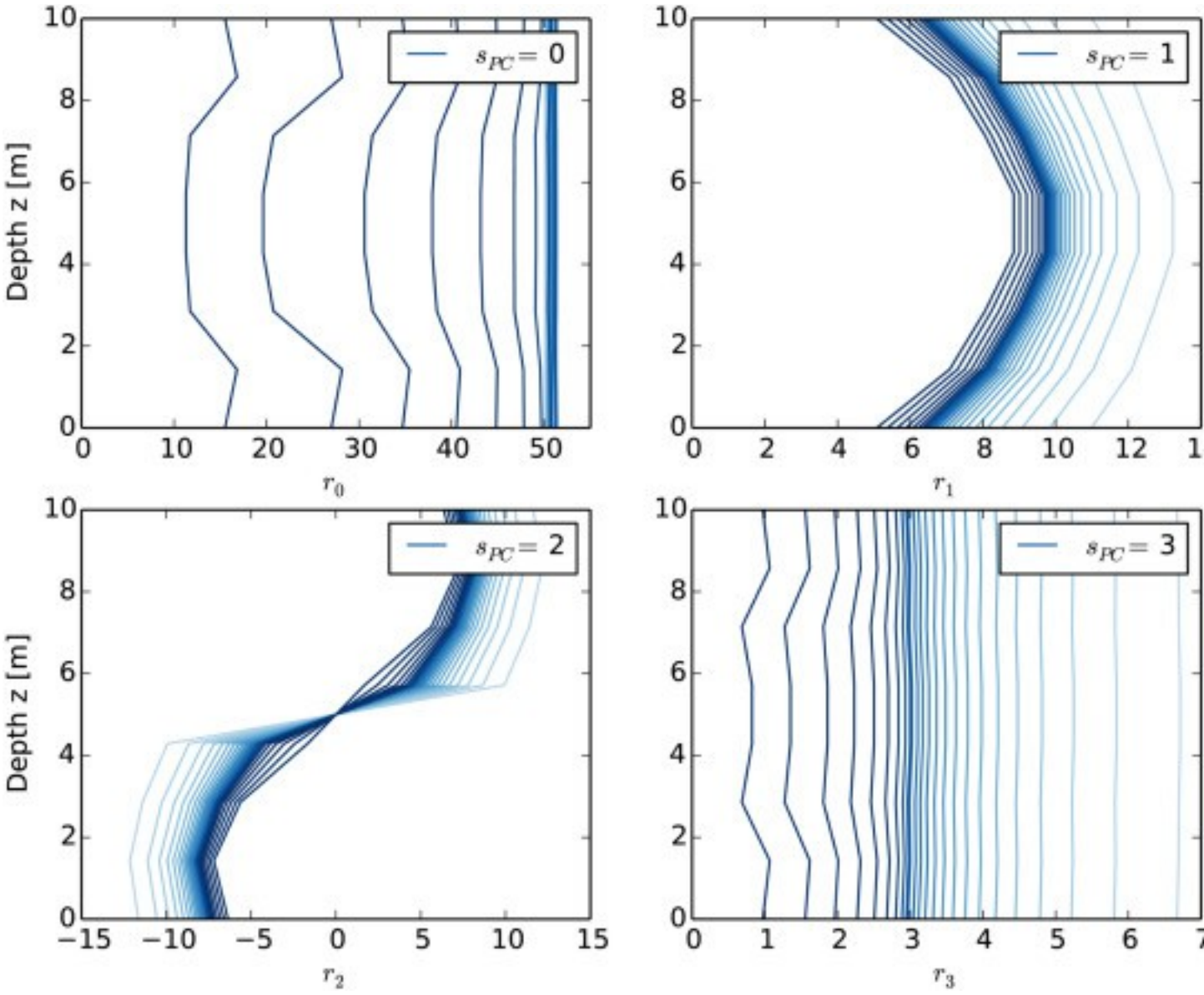

1. Download full-size image

Fig. 7. Evolution of the profile of PC coefficients of the linearized random shear stiffness along the depth of the shear beam (Case 1). (For interpretation of the references to color in this figure legend, the reader is referred to the web version of this article.)

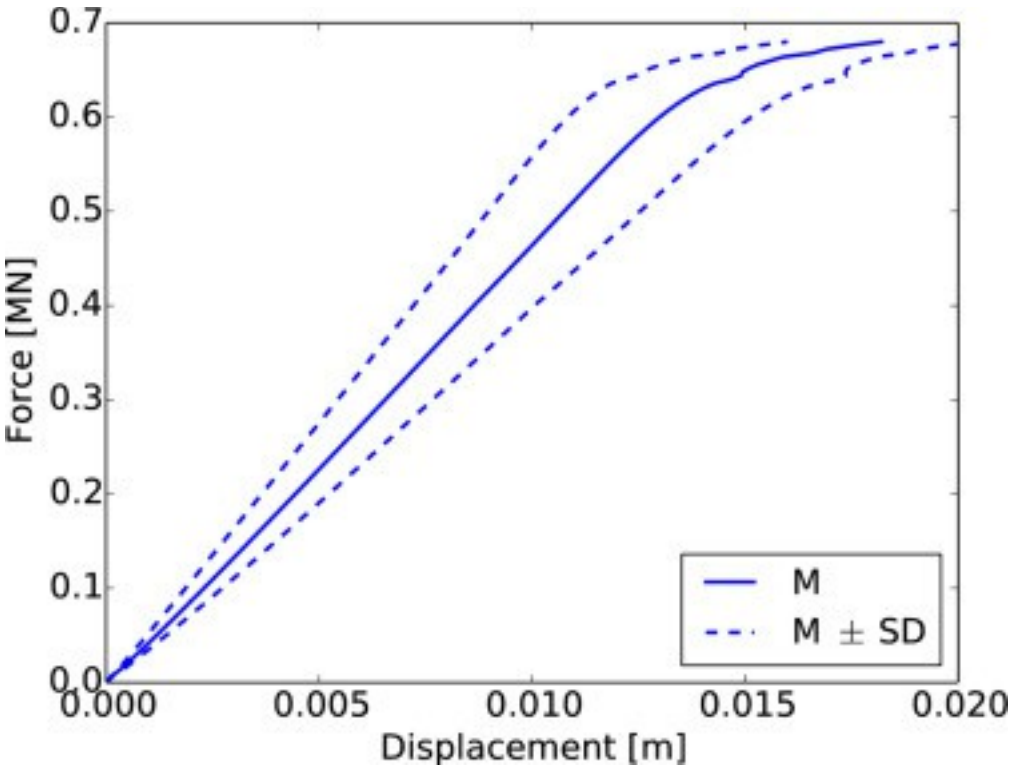

1. Download full-size image

Fig. 8. Force-mean (M) ± standard deviation (SD) of displacement response at the top of the shear column (Case 1).

Case 2 involves a more uncertain initial yield strength along with a deterministic hardening modulus, which results in the characteristic evolution of the PDF of shear strength at the top as shown in Fig. 9. Due to the large correlation length and small coefficient of variation of the shear modulus, the mean stress space is mostly active as well as the first stress space, which again is mostly diffusive. Fig. 10 shows the mean and standard deviation of the total stress versus the mean strain, at the same point, where a smooth transition to elastoplasticity is evident. The associated values of the PC coefficients are shown in Fig. 11, which again show a smooth decline of the governing coefficient due to the wide range of the elastoplastic transition. Fig. 12 shows the evolution of the profile of the PC coefficients of the linearized random stiffness similar to Case 1. Finally the global force–displacement response at the top of the shear beam is shown in Fig. 13, where we can identify a smooth transition to a linear hardening response.

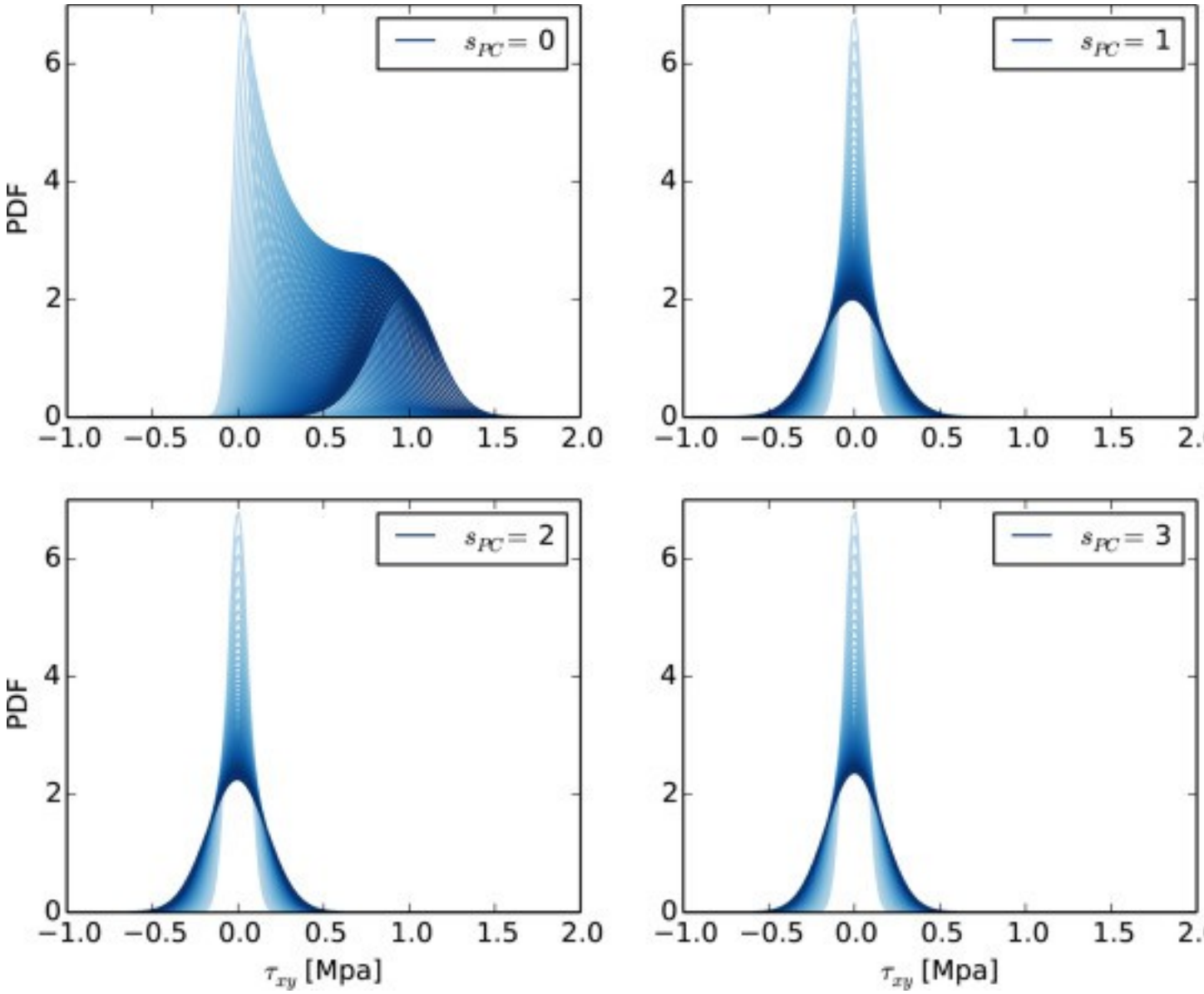

1. Download full-size image

Fig. 9. Evolution of the PDF of shear stress at the first 4 orthogonal KL/PC spaces (Case 2).

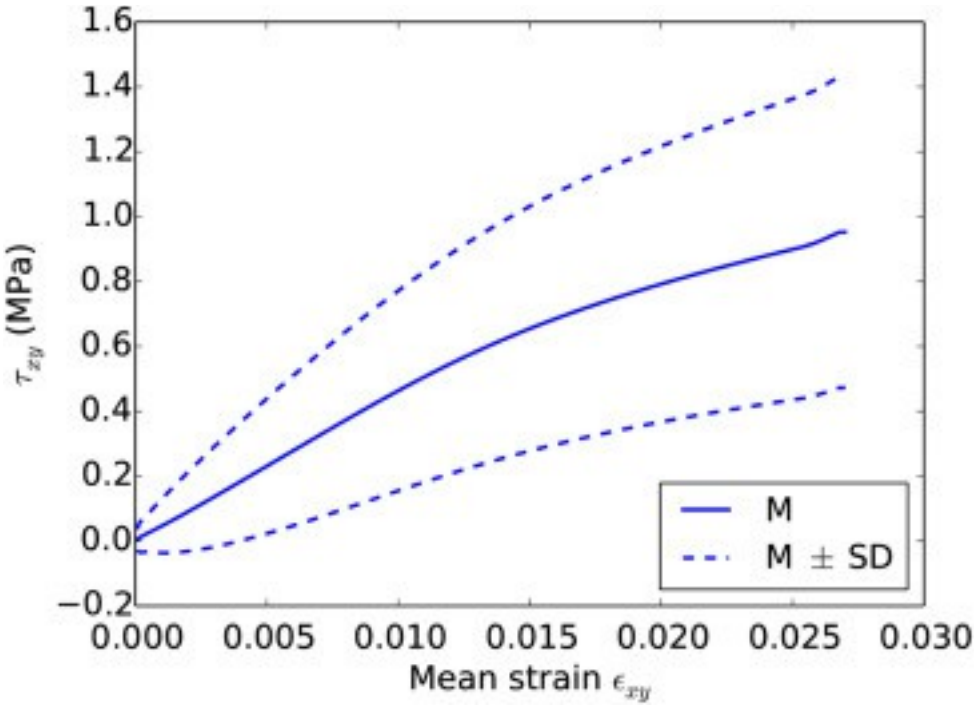

1. Download full-size image

Fig. 10. Mean (M) ± standard deviation (SD) of stress versus mean strain response at the top of the shear column (Case 2).

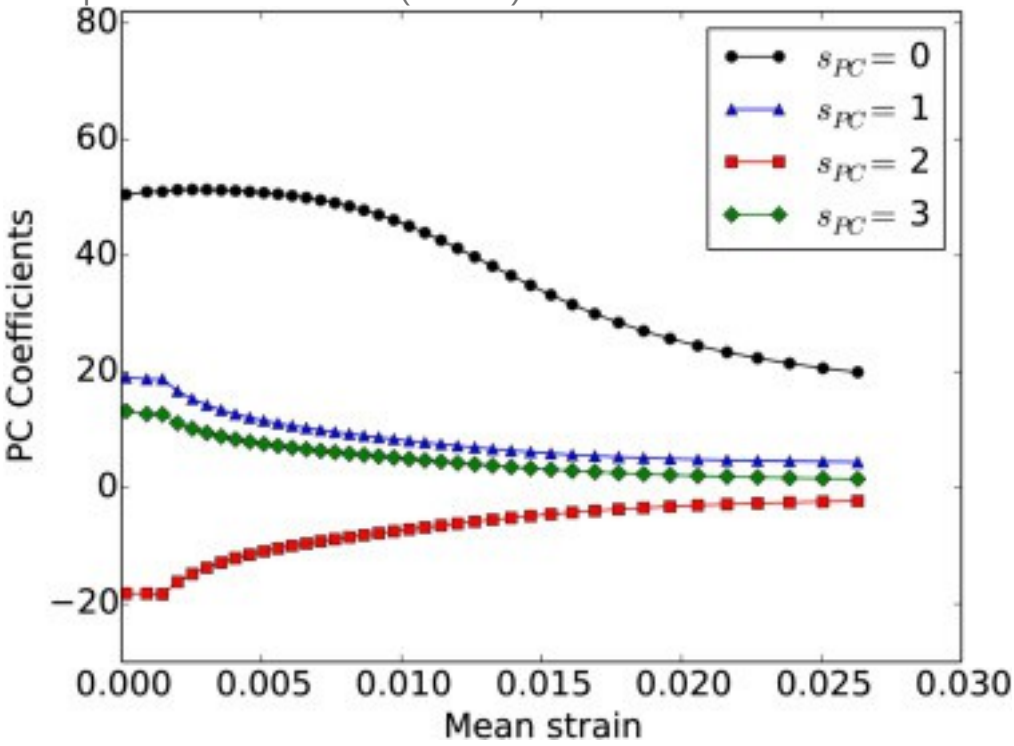

1. Download full-size image

Fig. 11. Evolution of PC coefficients of the linearized random shear stiffness (Case 2).

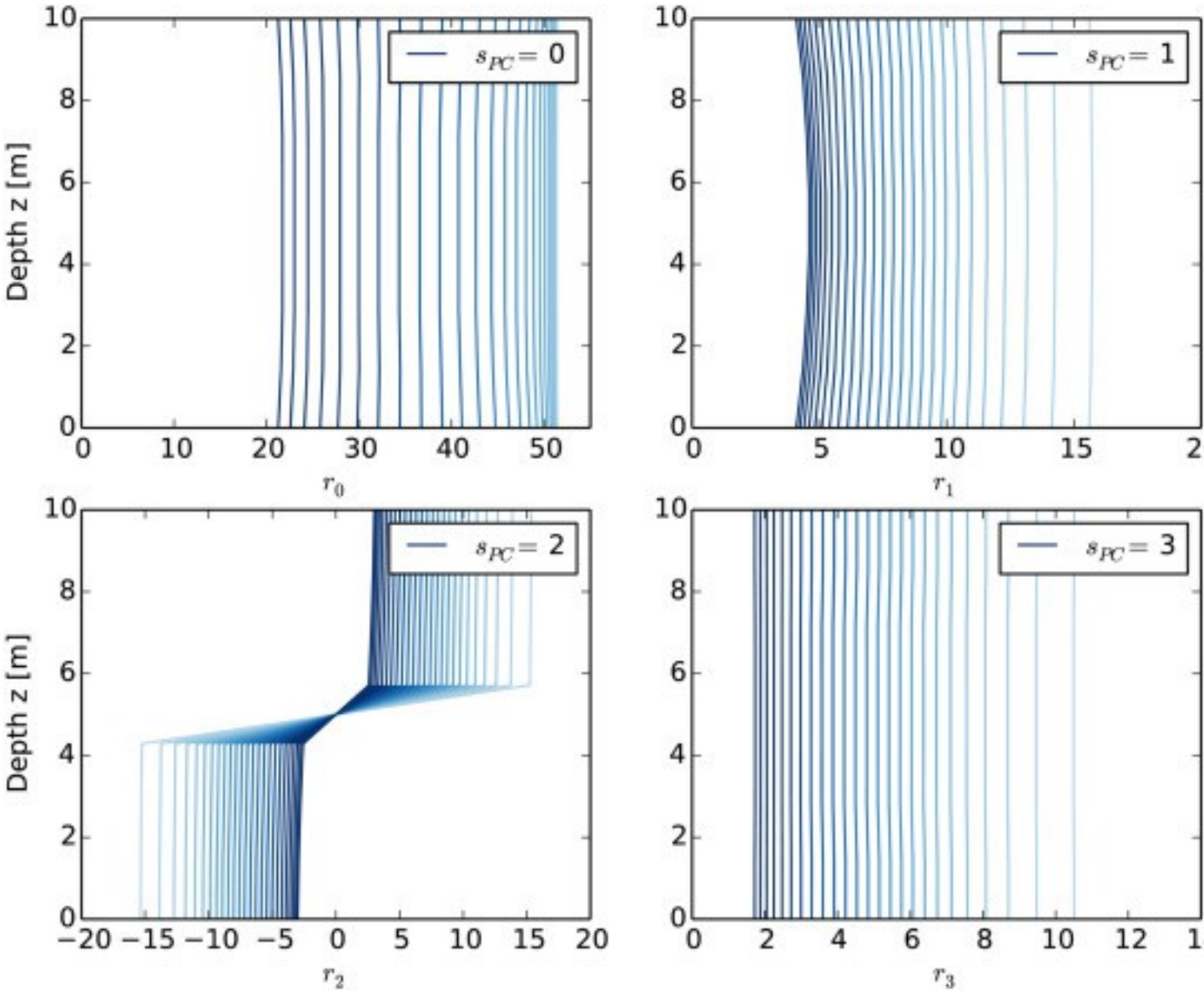

1. Download full-size image

Fig. 12. Evolution of the profile of PC coefficients of the linearized random shear stiffness along the depth of the shear beam (Case 2).

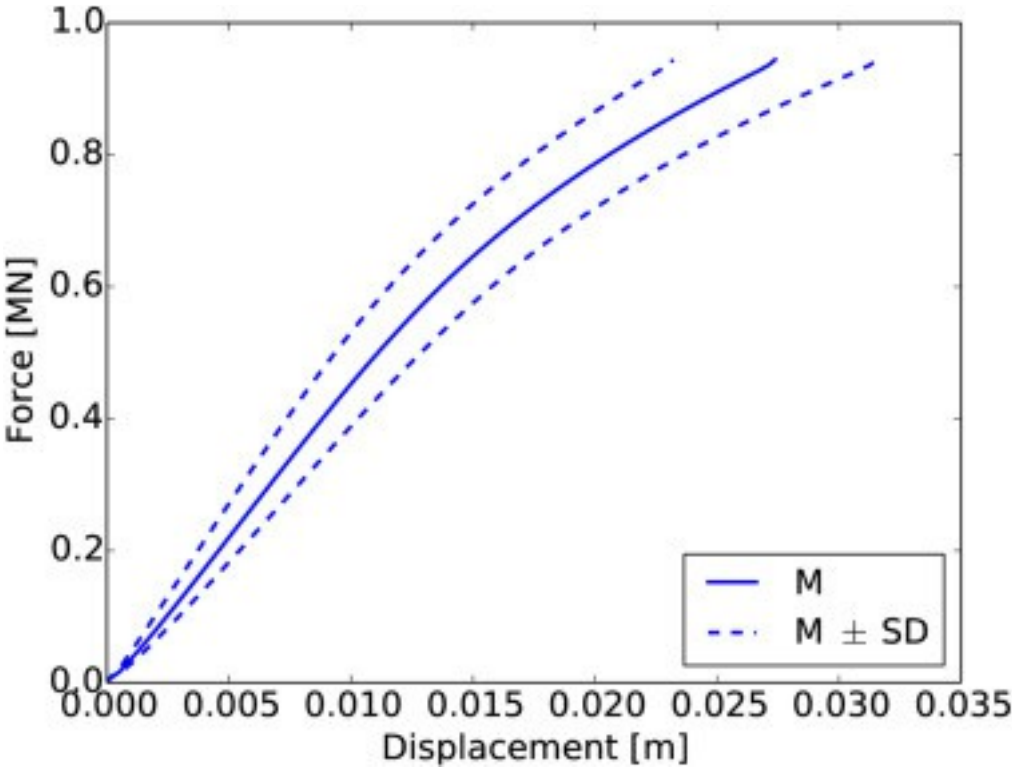

1. Download full-size image

Fig. 13. Force versus mean (M) ± standard deviation (SD) of displacement response at the top of the shear column (Case 2).

7. Conclusions

We have proposed a numerical technique to solve inelastic random boundary value problems based on stochastic Galerkin techniques and a nonlocal Fokker–Planck–Kolmogorov plasticity framework. It relies on a general linearization procedure that couples any functional representation of parametric uncertainty with an underlying advection–diffusion model describing its evolution. Being an intrusive framework it has the potential for higher convergence rates than conventional non-intrusive techniques, especially when combined with sparse PC representations and efficient FPK solution methods. An additional advantage of the framework is its potential for varying order of accuracy counterbalancing requirements in computation. Our numerical investigation of a simple shear beam problem yielded results that are consistent with the expected behavior in the elastoplastic regime. Further, the linearization procedure was able to effectively translate the evolution of the probability density functions in the FPK framework to the evolution of the PCE coefficients composing the elastoplastic stiffness. Future work will focus on the study of the accuracy of the proposed methodology and its comparison with non-intrusive techniques.

Acknowledgments

This work has been partly supported by the National Science Foundationunder Award No. 1200702 as well as the Department of Civil and Environmental Engineering of the University of California, Davis. We are grateful to the anonymous reviewers for their constructive comments.

References

[1]

G.A. Fenton**Random field modeling of CPT data**

ASCE J. Geotech. Geoenviron. Engrg., 125 (1999), pp. 486-498

CrossRefView Record in Scopus

[2]

K.-K. Phoon, F.H. Kulhawy**Characterization of geotechnical variability**

Can. Geotech. J., 36 (1999), pp. 612-624

CrossRefView Record in Scopus

[3]

A.L. Jones, S.L. Kramer, P. Arduino**Estimation of Uncertainty in Geotechnical Properties for Performance-Based Earthquake Engineering, Technical Report, PEER 2002/16**

Pacific Earthquake Engineering Research Center (2002)

[4]

G.I. Schüeller**A state-of-the-art report on computational stochastic mechanics**

Probab. Eng. Mech., 12 (1997), pp. 197-321

ArticleDownload PDF

[5]

H.G. Matthies, C.E. Brenner, C.G. Bucher, C. Guedes~Soares**Uncertainties in probabilistic numerical analysis of structures and soilds - stochastic finite elements**

Struct. Saf., 19 (1997), pp. 283-336

ArticleDownload PDFView Record in Scopus

[6]

I. Babuska, F. Nobile, R. Tempone**A stochastic collocation method for elliptic partial differential equations with random input data**

SIAM J. Numer. Anal., 45 (2007), pp. 1005-1034

CrossRefView Record in Scopus

[7]

D. Xiu**Fast numerical methods for stochastic computations**

Commun. Comput. Phys., 5 (2008), pp. 242-272

[8]

S. Acharjee, N. Zabaras**A non-intrusive stochastic Galerkin approach for modeling uncertainty propagation in deformation processes**
Comput. Struct., 85 (2007), pp. 244-254
ArticleDownload PDFView Record in Scopus

[9]

L. Giraldi, A. Litvinenko, D. Liu, H. Matthies, A. Nouy**To be or not to be intrusive? The solution of parametric and stochastic equations—the “plain vanilla” Galerkin case**
SIAM J. Sci. Comput., 36 (2014), pp. A2720-A2744
CrossRefView Record in Scopus

[10]

A. Keese**A Review of Recent Developments in the Numerical Solution of Stochastic Partial Differential Equations (Stochastic Finite Elements), Scientific Computing, 2003–06**
Deapartment of Mathematics and Computer Science, Technical University of Braunschweig, Brunswick, Germany (2003)

[11]

H. Matthies**Uncertainty Quantification with Stochastic Finite Elements**
Wiley (2004)

[12]

R.G. Ghanem, P.D. Spanos**Stochastic Finite Elements: A Spectral Approach**
Springer-Verlag (1991)
(Reissued by Dover Publications, 2003)

[13]

N. Wiener**The homogeneous chaos**
Amer. J. Math., 60 (1938), pp. 897-936
CrossRefView Record in Scopus

[14]

M.K. Deb, I.M. Babuska, J.T. Oden**Solution of stochastic partial differential equations using Galerkin finite element techniques**
Comput. Methods Appl. Mech. Eng., 190 (2001), pp. 6359-6372
ArticleDownload PDFView Record in Scopus

[15]

H.G. Matthies, A. Keese**Galerkin methods for linear and nonlinear elliptic stochastic partial differential equations**
Comput. Methods Appl. Mech. Eng., 194 (2005), pp. 1295-1331
ArticleDownload PDFView Record in Scopus

[16]

D. Xiu, G.E. Karniadakis**The Wiener–Askey polynomial chaos for stochastic differential equations**
SIAM J. Sci. Comput., 24 (2002), pp. 619-644
CrossRefView Record in Scopus

[17]

H.G. Matthies, A. Litvinenko, O. Pajonk, B.V. Rosić, E. Zander**Parametric and uncertainty computations with tensor product representations, in uncertainty quantification in scientific computing**
IFIP Adv. Inf. Commun. Technol., 377 (2012), pp. 139-150
CrossRefView Record in Scopus

[18]

A. Nouy, A. Cléent**eXtended stochastic finite element method for the numerical simulation of heterogeneous materials with random material interfaces**
Internat. J. Numer. Methods Engrg., 83 (2010), pp. 1312-1344
CrossRefView Record in Scopus

[19]

M. Anders, M. Hori**Three-dimensional stochastic finite element method for elasto-plastic bodies**
International Journal for Numerical Methods in Engineering, 51 (2001), pp. 449-478
CrossRefView Record in Scopus

[20]

B. Jeremić, K. Sett, M.L. Kavvas**Probabilistic elasto-plasticity: Formulation in 1–D**
Acta Geotech., 2 (2007), pp. 197-210
CrossRefView Record in Scopus

[21]

M.L. Kavvas**Nonlinear hydrologic processes: Conservation equations for determining their means and probability distributions**
J. Hydrol. Eng., 8 (2003), pp. 44-53
CrossRefView Record in Scopus

[22]

B. Jeremić, K. Sett**On probabilistic yielding of materials**
Commun. Numer. Methods. Eng., 25 (2009), pp. 291-300
CrossRefView Record in Scopus

[23]

K. Sett, B. Jeremić, M.L. Kavvas**Stochastic elastic–plastic finite elements**
Comput. Methods Appl. Mech. Eng., 200 (2011), pp. 997-1007
ArticleDownload PDFView Record in Scopus

[24]

B. Rosić**A Review of Computational Stochastic Elastoplasticity, Technical Report, Informatikbericht Nr. 2008-08**
Technische Universität, Braunschweig (2009)

[25]

M. Arnst, R. Ghanem**A variational-inequality approach to stochastic boundary value problems with inequality constraints and its application to contact and elastoplasticity**
International Journal for Numerical Methods in Engineering, 89 (2012), pp. 1665-1690
CrossRefView Record in Scopus

[26]

S. Sakamoto, R. Ghanem**Polynomial chaos decomposition for the simulation of non-Gaussian nonstationary stochastic processes**
J. Eng. Mech., 128 (2002), pp. 190-201
CrossRefView Record in Scopus

[27]

F. Benth, J. Gjerde**Convergence rates for finite element approximations for stochastic partial differential equations**
Stochastics: Int. J. Probab. Stoch. Rep., 63 (1998), pp. 313-326
CrossRefView Record in Scopus

[28]

C. Soize, R. Ghanem**Physical systems with random uncertainties: Chaos representations with arbitrary probability measure**
SIAM J. Sci. Comput., 26 (2004), pp. 395-410
CrossRef

[29]

M. Rosenblatt**Remarks on a multivariate transformation**
Ann. Math. Statist., 23 (1952), pp. 470-472
CrossRef

[30]

A. Nataf**Dètermination des distributions de probabilitès dont les marges sont donnèes**
C. R. Acad. Sci., 225 (1962), pp. 42-43

[31]

R. Ghanem**The nonlinear Gaussian spectrum of log-normal stochastic processes and variables**
J. Appl. Mech., 66 (1966), pp. 964-973

[32]

I. Babuska, P. Chatzipantelidis**On solving elliptic stochastic partial differential equations**
Comput. Methods Appl. Mech. Eng., 191 (2002), pp. 4093-4122
ArticleDownload PDFView Record in Scopus

[33]

R. Courant, D. Hilbert**Methods of Mathematical Physics**
Wiley (1989)

[34]

K. Phoon, S. Huang, S. Quek**Implementation of Karhunen–Loeve expansion for simulation using a wavelet–Galerkin scheme**
Probab. Eng. Mech., 17 (2002), pp. 293-303
ArticleDownload PDFView Record in Scopus

[35]

B. Khoromskij, A. Litvinenko, H. Matthies**Application of hierarchical matrices for computing the Karhunen–Loève expansion**
Computing, 84 (2009), pp. 49-67
CrossRefView Record in Scopus

[36]

S. Rahman, H. Xu**A meshless method for computational stochastic mechanics**
Int. J. Comput. Methods Eng. Sci. Mech., 6 (2005), pp. 41-58
CrossRefView Record in Scopus

[37]

A. Der~Kiureghian, B.J. Ke**The stochastic finite element method in structural reliability**
J. Probab. Eng. Mech., 3 (1988), pp. 83-91
ArticleDownload PDFView Record in Scopus

[38]

C.-C. Li, A. Der~Kiureghian**Optimal discretization of random fields**
ASCE J. Eng. Mech., 119 (1993), pp. 1136-1154
CrossRefView Record in Scopus

[39]

T. Melink, J. Korelc**Stability of Karhunen–Loeve expansion for the simulation of gaussian stochastic fields using galerkin scheme**
Probab. Eng. Mech., 37 (2014), pp. 7-15
ArticleDownload PDFView Record in Scopus

[40]

T. Hughes**The Finite Element Method: Linear Static and Dynamic Finite Element Analysis**
Prentice Hall Inc. (1987)

[41]

Wolfram Research Inc.**Mathematica Version 5.0**
Wolfram Research Inc., Champaign, Illonois (2003)

[42]

R. Ghanem, R.M. Kruger**Numerical solution of spectral stochastic finite element systems**
Comput. Methods Appl. Mech. Eng., 129 (1996), pp. 289-303
ArticleDownload PDFView Record in Scopus

[43]
E. Ullmann**Solution strategies for stochastic finite element discretizations**
(Doctoral dissertation)
TU Bergakademie, Freiberg (2008)

[44]
O.L. Maitre, O.M. Knio**Spectral Methods for Uncertainty Quantification with Applications to Computational Fluid Dynamics**
Springer, Dordrecht (2010)

[45]
D. Ghosh, P. Avery, C. Farhat**A FETI-preconditioned conjugate gradient method for large-scale stochastic finite element problems**
International Journal for Numerical Methods in Engineering, 80 (2009), pp. 914-931
CrossRefView Record in Scopus

[46]
K. Levenberg**A method for the solution of certain non-linear problems in least squares**
Quart. Appl. Math., 2 (1944), pp. 164-168
CrossRefView Record in Scopus

$$D(\mathbf{x},\theta)=\sum_{i=0}^{M} r_i(\mathbf{x})\,\Phi_i[\{\xi_r(\theta)\}] \tag{1}$$

where $\Phi_i[\{\xi_r(\theta)\}]$ is a set of Hermite polynomials of an underlying Gaussian set $\xi_r(\theta)$ and θ is an element of the space of random variables Ω. The variable M denotes the order of the PCE. It can be shown that the latter is convergent in $L_2(\Omega)$; a relevant convergence rate study can be found in [27].

The spatially dependent coefficients r_i may be computed via simple projection but this kind of expansion is defined without any reference to the random field $D(\mathbf{x},\theta)$ and the expected accuracy is low. Therefore, a correlation structure is endowed to the underlying field by considering the following multidimensional PC representation:

$$D(\mathbf{x},\theta)=\sum_{i=0}^{M} D_i(\mathbf{x})\,\Gamma_i[(\mathbf{x},\theta)] \tag{2}$$

where $\Gamma_i[\mathbf{x},\theta]$ is now a set of multidimensional Hermite polynomials of an underlying correlated Gaussian field $\gamma(\mathbf{x},\theta)$. The orthogonality of the polynomials is employed to calculate the coefficients $D_i(\mathbf{x})$ as:

$$D_i(\mathbf{x})=\frac{\langle D\Gamma_i\rangle}{\langle\Gamma_i^2\rangle} \tag{3}$$

where the numerator can be evaluated with the inverse CDF approach using some type of numerical quadrature (e.g., collocation, Monte Carlo (MC), quasi Monte Carlo (QMC), etc.). The correlation function ρ_D of $\gamma(\mathbf{x},\theta)$ induced on $D(\mathbf{x},\theta)$ is given as the solution to the following polynomial equation [26]:

$$\rho_D(\mathbf{x}_1,\mathbf{x}_2)=\sum_{i=1}^{M} D_i(\mathbf{x}_1)\,D_i(\mathbf{x}_2)\,i!\langle\gamma(\mathbf{x}_1)\,\gamma(\mathbf{x}_2)\rangle^i \tag{4}$$

$$\gamma(\mathbf{x},\theta)=\sum_{i=1}^{Q}\sqrt{\lambda_i}f_i(\mathbf{x})\xi_i(\theta) \tag{6}$$

subject to the following constraint deriving from the unit variance condition imposed on $\gamma(\mathbf{x})$:

$$\sum_{i=1}^{Q}\left(\sqrt{\lambda_i}f_i(\mathbf{x})\right)^2=1. \tag{7}$$

In the above equations, λ_i and $f_i(\mathbf{x})$ denote the resulting eigenvalues and eigenvectors respectively, and Q denotes the dimensionality of the truncated expansion. It is required that we re-normalize to a unit variance as follows:

$$\gamma(\mathbf{x},\theta)=\sum_{i=1}^{Q}\frac{\sqrt{\lambda_i}f_i(x)}{\sqrt{\sum_{m=1}^{Q}\left(\sqrt{\lambda_m}f_m(\mathbf{x})\right)^2}}\xi_i(\theta). \tag{8}$$

By equating the two representations of $D(\mathbf{x},\theta)$ in Eqs. (1), (2), we can find the coefficients $r_i(x)$ as

$$r_i(\mathbf{x})=\frac{p!}{\langle\Phi_i^2\rangle}D_p(\mathbf{x})\prod_{j=1}^{p}\frac{\sqrt{\lambda_{k(j)}}f_{k(j)}(\mathbf{x})}{\sqrt{\sum_{m=1}^{Q}\left(\sqrt{\lambda_m}f_m(\mathbf{x})\right)^2}} \tag{9}$$

$$D(\mathbf{x}) = e^{g(\mathbf{x})} \tag{10}$$

with the following mean and variance relations:

$$\bar{D} = e^{\bar{g}} \tag{11}$$

$$\sigma_D = e^{\sigma_g}. \tag{12}$$

The process $g(\mathbf{x})$ is expanded in the Karhunen–Loève sense as:

$$g(\mathbf{x}) = \bar{g} + \sum_{i=1}^{N} g_i \xi_i = \bar{g} + \sum_{i=1}^{N} \sqrt{\lambda_i} f_i(\mathbf{x}) \xi_i \tag{13}$$

and projection into polynomial chaos yields analytical coefficients $r_i(\mathbf{x})$:

$$r_i(\mathbf{x}) = \frac{\langle e^g \Phi_i \rangle}{\langle \Phi_i^2 \rangle} = \frac{\prod_{j=1}^{p} \sqrt{\lambda_{k(j)}} f_{k(j)}(\mathbf{x})}{\langle \Phi_i^2 \rangle} e^{\bar{g} + \frac{1}{2} \sum_{j=1}^{N} g_j^2}. \tag{14}$$

$$S_u(\mathbf{x},\theta) = \bar{S}_u(\mathbf{x}) + \sum_{i=1}^{N} \sqrt{\lambda_i} f_i(\mathbf{x}) \xi_i(\theta) \tag{15}$$

by considering the following Fredholm integral equation of the second kind [33] with the covariance function C_{S_u} as a kernel:

$$\int_D C_{S_u}(\mathbf{x}_1,\mathbf{x}_2) f_k(\mathbf{x}_1) d\mathbf{x}_1 = \lambda_k f_k(\mathbf{x}_2). \tag{16}$$

This expansion is optimal in the sense that it is the best approximation that may be achieved in the $L_2(D) \otimes L_2(\Omega)$ norm.

In some cases (e.g., triangular, exponential kernel) the above eigenproblem may be solved analytically, but in the general case a numerical approximation scheme is required. In that sense, a number of methods have been applied including FEM [12], wavelet-Galerkin [34], $\mathscr{H}$-matrices [35] and meshless methods [36].

In a standard finite element setting, each eigenfunction, f_k of the kernel is approximated as:

$$f_k(\mathbf{x}) = \sum_{i=1}^{N} d_{ik} h_i(\mathbf{x}) \tag{17}$$

where h and d represent basis functions of compact support and appropriate nodal coefficients, respectively. Utilizing the above representation and requiring the error to be orthogonal to the approximating space, one may transform Eq. (16) to the following weak form:

$$\sum_{i=1}^{N} d_{ik} \left[\int_D \int_D C_{S_u}(\mathbf{x}_1,\mathbf{x}_2) h_i(\mathbf{x}_2) h_j(\mathbf{x}_1) d\mathbf{x}_1 d\mathbf{x}_2 - \lambda_k \int_D h_i(\mathbf{x}) h_j(\mathbf{x}) d\mathbf{x} \right] = 0. \tag{18}$$

$$u(\mathbf{x},\theta)=\sum_{i=0}^{P} d_i(\mathbf{x})\,\Psi_i\left[\xi_r(\theta)\right] \tag{19}$$

where $\Psi_i\left[\xi_r(\theta)\right]$ represents a set of random Hermite polynomials of order P. The component $d_i(\mathbf{x})$ is, then, further discretized in the spatial sense using standard finite element shape functions:

$$d_i(\mathbf{x})=\sum_{j=1}^{N} d_{ij}N_j(\mathbf{x})\,. \tag{20}$$

This results in a final expression for the random displacement field:

$$u(\mathbf{x},\theta)=\sum_{i=0}^{P}\sum_{j=1}^{N} d_{ij}N_j(\mathbf{x})\,\Psi_i\left[\xi_r(\theta)\right]. \tag{21}$$

4. Finite element formulation

Employing the Galerkin weak formulation of linearized static FEM [40], we have the following simplified form :

$$\sum_e\left[\int_{D_e}\nabla N_m(\mathbf{x})\,D(\mathbf{x},\theta)\,\nabla N_n(\mathbf{x})\,dV\,u_n-\int_{D_e}f_m(\mathbf{x},\theta)\,dV\right]=0 \tag{22}$$

where $\sum_e$ denotes the assembly procedure over all finite elements of the discretized domain V and $f_m(\mathbf{x})$ incorporates the various elemental contributions to the global force vector.

Combining Eqs. (1), (21), (22) and denoting the shape function gradients as:

$$\nabla N_n(\mathbf{x}) \coloneqq B_n(\mathbf{x}) \tag{23}$$

yields:

$$\sum_e \left[\int_{D_e} B_m(\mathbf{x}) \sum_{i=0}^{M} r_i(\mathbf{x}) \Phi_i \left[\{\xi_r(\theta)\} \right] B_n(\mathbf{x}) \sum_{j=0}^{P} \sum_{k=0}^{P} d_{nj} \Psi_j \left[\xi_r(\theta) \right] \Psi_k \left[\xi_r(\theta) \right] dV - \int_{D_e} \sum_{k=0}^{P} f_m(\mathbf{x}, \theta) \Psi_k \left[\xi_r(\theta) \right] dV \right] = 0. \tag{25}$$

Taking expectation on both sides results in the following system of equations:

$$\sum_{n=1}^{N} \sum_{j=0}^{P} d_{nj} \sum_{k=1}^{M} b_{ijk} K_{mni} = F_m \left\langle \Psi_k \left[\{\xi_r\} \right] \right\rangle \tag{26}$$

where

$$K_{mni} = \int_D B_m(\mathbf{x}) r_i(\mathbf{x}) B_n(\mathbf{x}) dV \tag{27}$$

and

$$F_m = \int_D f_m(\mathbf{x}, \theta) dV. \tag{28}$$

Symbolic manipulations are carried out using Mathematica [41] in order to precompute the coefficients of the tensor:

$$b_{ijk} = \left\langle \Phi_i \left[\{\xi_r\} \right] \Psi_j \left[\{\xi_r\} \right] \Psi_k \left[\{\xi_r\} \right] \right\rangle. \tag{29}$$

$$\frac{d\sigma_{ij}(x_t,t)}{dt} = D_{ijkl}\left(x_t,t\right)\frac{d\epsilon_{kl}(x_t,t)}{dt} \tag{30}$$

where $D_{ijkl}\left(x_t,t\right)$ is the continuum stiffness tensor, evaluated at the spatial coordinate x_t, and can be either elastic or elasto-plastic:

$$D_{ijkl} = \begin{cases} D^{el}_{ijkl}; & f<0 \vee (f=0 \wedge df<0) \\ D^{el}_{ijkl} - \frac{D^{el}_{ijmn}\frac{\partial U}{\partial \sigma_{mn}}\frac{\partial f}{\partial \sigma_{pq}}D^{el}_{pqkl}}{\frac{\partial f}{\partial \sigma_{rs}}D^{el}_{rstu}\frac{\partial U}{\partial \sigma_{tu}} - \frac{\partial f}{\partial q_*}r_*}; & f=0 \wedge df<0 \end{cases} \tag{31}$$

according to the established Karush–Kuhn–Tucker conditions.

In the above equation, D^{el}_{ijkl} is the elastic stiffness tensor, f is the yield function, which is a function of stress σ_{ij} and internal variables q_* (scalar, vector- or tensor-valued), while U is the plastic potential function. In its most general form, the incremental constitutive equation takes the form

$$\frac{d\sigma_{ij}(x_t,t)}{dt} = \beta_{ijkl}\left(\sigma_{ij}, D_{ijkl}, q_*, r_*; x_t, t\right)\frac{d\epsilon_{kl}(x_t,t)}{dt} \tag{32}$$

or

$$\frac{d\sigma_{ij}(x_t,t)}{dt} = \eta_{ijkl}\left(\sigma_{ij}, D_{ijkl}, \epsilon_{kl}\left(x_t,t\right)q_*, r_*; x_t, t\right) \tag{33}$$

(34)

$$\frac{\partial P(\sigma_{ij},t)}{\partial t} =$$
$$-\frac{\partial}{\partial \sigma_{mn}}\left[\left\{\left\langle \eta_{mn}\left(\sigma_{mn}\left(t\right),D_{mnrs},\epsilon_{rs}\left(t\right)\right)\right\rangle +\right.\right.$$
$$\left.\left.\int_0^t d\tau Cov_0\left[\frac{\partial \eta_{mn}(\sigma_{mn}(t),D_{mnrs},\epsilon_{rs}(t))}{\partial \sigma_{ab}};\eta_{ab}\left(\sigma_{ab}\left(t-\tau\right),D_{abcd},\epsilon_{cd}\left(t-\tau\right)\right)\right]\right\} P\left(\sigma_{ij}\left(t\right),\right.$$
$$+\frac{\partial^2}{\partial \sigma_{mn}\partial \sigma_{ab}}\left[\right.$$
$$\left.\int_0^t d\tau Cov_0\left[\eta_{mn}\left(\sigma_{mn}\left(t\right),D_{mnrs},\epsilon_{rs}\left(t\right)\right);\eta_{ab}\left(\sigma_{ab}\left(t-\tau\right),D_{abcd},\epsilon_{cd}\left(t-\tau\right)\right)\right] P\left(\sigma\right.\right.$$

where $P\left(\sigma_{ij},t\right)$ is the probability density of stress, $\langle\cdot\rangle$ is the expectation operator, $Cov_0\left[\cdot\right]$ is the time-ordered covariance operator and η_{ij} is a generalized random tensor operator. Details of this derivation can be found in [20]. The above equation is equivalent to the following generalized form:

(35)

$$\frac{\partial P(\sigma_{ij},t)}{\partial t} = -\frac{\partial}{\partial \sigma_{mn}}\left[N^{\sigma^{eq}}_{(1)_{mn}} P\left(\sigma_{ij},t\right) - \frac{\partial}{\partial \sigma_{ab}}\left\{N^{\sigma^{eq}}_{(2)_{mnab}} P\left(\sigma_{ij},t\right)\right\}\right]$$

where $N_{(1)}$ and $N_{(2)}$ are advection and diffusion coefficients respectively that are particular to the constitutive model. Given the initial and boundary conditions as well as the second-order statistics of material properties, Eq. (35) may be solved with second-order accuracy.

To account for the uncertainty in the probabilistic yielding, Jeremić and Sett [22] introduced the following equivalent advection and diffusion coefficients:

$$N^{\sigma^{eq}}_{(1)_{mn}}\left(\sigma_{ij}\right) = \left(1 - P\left[f>0\right]\right) N^{el}_{(1)_{mn}} + P\left[f>0\right] N^{ep}_{(1)_{mn}} \quad (36)$$

(37)

$$N^{el}_{(1)_{mn}} = \left\langle D^{el}_{mnrs}\dot{\epsilon}_{rs} \right\rangle \tag{38}$$

$$N^{el}_{(2)_{mnab}} = t\mathrm{Cov}_0\left[D^{el}_{mnrs}\dot{\epsilon}_{rs}; D^{el}_{abcd}\dot{\epsilon}_{cd}\right] \tag{39}$$

and

$$N^{ep}_{(1)_{mn}} = \langle D^{ep}_{mnrs}\dot{\epsilon}_{rs}\rangle + \int_0^t d\tau Cov_0\left[\frac{\partial}{\partial\sigma_{ab}}\{D^{ep}_{mnrs}\dot{\epsilon}_{rs}\}; D^{ep}_{abcd}\dot{\epsilon}_{cd}\right] \tag{40}$$

$$N^{ep}_{(2)_{mnab}} = \int_0^t d\tau Cov_0\left[D^{ep}_{mnrs}(t)\,\dot{\epsilon}_{rs}; D^{ep}_{abcd}(t-\tau)\,\dot{\epsilon}_{cd}\right]. \tag{41}$$

The evolution of any internal variable $\mathbf{q}_i$ of the model is handled through a coupled FPK equation of the form:

$$\frac{\partial\widetilde{P}(q_i,t)}{\partial t} = -\frac{\partial}{\partial q_m}\left[N^{q^{ep}}_{(1)_m}(\sigma_{mn},q_m)\,\widetilde{P}(q_i,t) - \frac{\partial}{\partial q_n}\left\{N^{q^{ep}}_{(2)_{mn}}(\sigma_{mn},q_m)\,\widetilde{P}(q_i,t)\right\}\right]. \tag{42}$$

The advection and diffusion coefficients in the above equation are given similar to Eqs. (36), (36) but with no contributions of any "elastic" state:

$$N^{q^{ep}}_{(1)_m}(\sigma_{ij},q_i) = P[f>0]\; N^{q^{ep}}_{(1)_m} \tag{43}$$

$$N^{q^{ep}}_{(2)_{mn}}(\sigma_{ij},q_i) = P[f>0]\; N^{q^{ep}}_{(2)_{mn}}. \tag{44}$$

The elastoplastic components of the equivalent advection and diffusion terms are functions of the so-called loading index or plastic multiplier L and the rates of evolution of the internal variables r_i:

$$N^{q^{ep}}_{(1)_m} = \langle Lr_i\rangle + \int_0^t d\tau\mathrm{Cov}_0\left[\frac{\partial}{\partial q_j}Lr_i(t); Lr_j(t-\tau)\right] \tag{45}$$

$$N^{q^{ep}}_{(2)_{mn}} = \int_0^t d\tau\mathrm{Cov}_0\left[Lr_i(t); Lr_j(t-\tau)\right] \tag{46}$$

$$N^{s^{eq}}_{(1)_{mn}}\left(\sigma^s_{ij},\mathbf{x}\right)=\left(1-P\left[f>0\right]\right)\,N^{el}_{(1)_{mn}}+P\left[f>0\right]\,N^{ep}_{(1)_{mn}} \tag{48}$$

$$N^{s^{eq}}_{(2)_{mnab}}\left(\sigma^s_{ij},\mathbf{x}\right)=\left(1-P\left[f>0\right]\right)\,N^{el}_{(2)_{mnab}}+P\left[f>0\right]\,N^{ep}_{(2)_{mnab}}. \tag{49}$$

For the purposes of this study, let us consider an isotropic linear elastic—Mises isotropic hardening model and derive the equivalent advection and diffusion coefficients for this case. The isotropic linear elasticity tensor in Eq. (31) reads:

$$D^{el}_{ijkl}=G\delta_{ik}\delta_{jl}+\left(K-\tfrac{2}{3}G\right)\delta_{ij}\delta_{kl} \tag{50}$$

where K and G denote the bulk and shear modulus respectively and are represented as random fields (see for example Eq. (1)).

The elastoplastic continuum tangent tensor in Eq. (31) is given in the following general form:

$$D^{ep}_{ijkl}=G\delta_{ik}\delta_{jl}+\left(K-\tfrac{2}{3}G\right)\delta_{ij}\delta_{kl}-\frac{A_{ij}A^*_{kl}}{B+K_P}. \tag{51}$$

The Mises linear hardening yield function is written as:

$$f=\sqrt{J_2}-S_u=\sqrt{\tfrac{1}{2}s_{ij}s_{ij}}-S_u. \tag{52}$$

Under the assumption of associated flow rule we have:

$$\frac{\partial f}{\partial\sigma_{ij}}=\frac{\partial U}{\partial\sigma_{ij}} \tag{53}$$

which results in the following symmetry:

$$\frac{\partial f}{\partial\sigma_{ij}}=\frac{\partial f}{\partial\sigma_{ij}} \tag{54}$$

$$S_u = S_u\left(\epsilon_{eq}^p\right). \tag{56}$$

After imposing the consistency condition, we have:

$$K_P = -\frac{\partial f}{\partial S_u}\bar{k} = -\frac{1}{\sqrt{3}}\frac{\partial f}{\partial S_u}\frac{dS_u}{d\epsilon_{eq}^p}\frac{\partial f}{\partial \sqrt{J_2}} = \frac{1}{\sqrt{3}}\frac{dS_u}{d\epsilon_{eq}^p}. \tag{57}$$

Combining Eqs. (36)–(41), (50)–(51), we can derive the final coefficients of the FPK constitutive rate equation as:

$$\begin{aligned}
&N_{(1)_{mn}}^{s^{eq}} = \left(1 - P\left[f > 0\right]\right)\left\langle\left[G\delta_{mr}\delta_{ns} + \left(K - \tfrac{2}{3}G\right)\delta_{mn}\delta_{rs}\right]\dot{\epsilon}_{rs}\left(t\right)\right\rangle \\
&+ P\left[f > 0\right] \\
&\left\langle\left[G\delta_{mr}\delta_{ns} + \left(K - \tfrac{2}{3}G\right)\delta_{mn}\delta_{rs} - \frac{1}{G + \frac{1}{\sqrt{3}}\frac{dS_u}{d\epsilon_{eq}^p}}\left(\frac{G}{\sqrt{J_2}}\right)^2 s_{ij}^s\left(t\right)s_{kl}^s\left(t\right)\right]\dot{\epsilon}_{rs}\left(t\right)\right\rangle \\
&+ \int_0^t d\tau Cov_0 \\
&\left[\frac{\partial}{\partial \sigma_{ab}^s}\left\{\left[G\delta_{mr}\delta_{ns} + \left(K - \tfrac{2}{3}G\right)\delta_{mn}\delta_{rs} - \frac{1}{G + \frac{1}{\sqrt{3}}\frac{dS_u}{d\epsilon_{eq}^p}}\left(\frac{G}{\sqrt{J_2}}\right)^2 s_{ij}^s\left(t\right)s_{kl}^s\left(t\right)\right]\dot{\epsilon}_{rs}\left(t\right)\right.\right. \\
&\left.\left.\left[G\delta_{ac}\delta_{bd} + \left(K - \tfrac{2}{3}G\right)\delta_{ab}\delta_{cd} - \frac{1}{G + \frac{1}{\sqrt{3}}\frac{dS_u}{d\epsilon_{eq}^p}}\left(\frac{G}{\sqrt{J_2}}\right)^2 s_{ab}^s\left(t-\tau\right)s_{cd}^s\left(t-\tau\right)\right]\dot{\epsilon}_{cd}\left(t-\right.\right.\right.
\end{aligned} \tag{58}$$

$$\begin{aligned}
&N_{(2)_{mnab}}^{s^{eq}} = \left(1 - P\left[f > 0\right]\right)t \\
&\mathrm{Cov}_0\left[\left\{G\delta_{mr}\delta_{ns} + \left(K - \tfrac{2}{3}G\right)\delta_{mn}\delta_{rs} - \frac{1}{G + \frac{1}{\sqrt{3}}\frac{dS_u}{d\epsilon_{eq}^p}}\left(\frac{G}{\sqrt{J_2}}\right)^2 s_{ij}^s\left(t\right)s_{kl}^s\left(t\right)\right\}\dot{\epsilon}_{rs}\left(t\right)\right. \\
&\left.\left[G\delta_{ac}\delta_{bd} + \left(K - \tfrac{2}{3}G\right)\delta_{ab}\delta_{cd} - \frac{1}{G + \frac{1}{\sqrt{3}}\frac{dS_u}{d\epsilon_{eq}^p}}\left(\frac{G}{\sqrt{J_2}}\right)^2 s_{ab}^s\left(t\right)s_{cd}^s\left(t\right)\right]\dot{\epsilon}_{cd}\left(t\right)\right] \\
&+ P\left[f > 0\right] \\
&\left[\left(\right.\right.
\end{aligned} \tag{59}$$

$$\frac{\partial P^{lin}\left(\sigma_{ij}^{s},t\right)}{\partial t}=-N_{(1)_{mn}}^{s^{lin}}\frac{\partial P\left(\sigma_{ij}^{s},t\right)}{\partial\sigma_{mn}^{s}}+N_{(2)_{mnab}}^{s^{lin}}\frac{\partial^{2}P\left(\sigma_{ij}^{s},t\right)}{\partial\sigma_{mn}^{s}\sigma_{ab}^{s}} \tag{60}$$

where the linearized advection and diffusion coefficients are given by:

$$N_{(1)_{mn}}^{s^{lin}}=r_{mnab}^{s^{(k)}}\sum_{i=0}^{P}\left\langle \Phi_{i}\Psi_{s}\right\rangle \frac{1}{2\Delta t} \tag{61}$$

$$\sum_{j=1}^{N}\left[N_{j,b}\left(\mathbf{x}\right)\Delta d_{ija}^{k-1}+N_{j,a}\left(\mathbf{x}\right)\Delta d_{ijb}^{k-1}\right]$$

$$N_{(2)_{mnab}}^{s^{lin}}=t\left(r_{mnab}^{s^{(k)}}\right)^{2} \tag{62}$$

$$\sum_{i=0}^{P}\mathrm{Var}\left[\Phi_{i}\Psi_{s}\right]\frac{1}{4\Delta t^{2}}\left[N_{j,b}\left(\mathbf{x}\right)\Delta d_{ija}^{k-1}+N_{j,a}\left(\mathbf{x}\right)\Delta d_{ijb}^{k-1}\right]^{2}.$$

In an explicit scheme, the strain increment at the $(k-1)$th step is utilized, while the fourth-order tensor valued PC coefficient $r_{mnab}^{s^{(k)}}$ is unknown. Depending on the specific constitutive model, the above equations may be simplified to include scalar PC coefficients and deterministic bases in an appropriate tensor format. Combining Eqs. (35), (60), one ends up with an over-determined residual system of equations in terms of the unknown coefficients at time step k:

$$R_{i}\left(r_{mnab}^{s^{(k)}}\right)=\frac{\partial P^{\mathrm{lin}}(\boldsymbol{\sigma}_{i}^{s},t)}{\partial t}-\frac{\partial P(\boldsymbol{\sigma}_{i}^{s},t)}{\partial t}=0,\quad i=1,\ldots,N. \tag{63}$$

$$\frac{\partial P^{lin}(\sigma_{ij},t)}{\partial t} = -N^{lin}_{(1)} \frac{\partial P(\sigma_{ij},t)}{\partial \sigma_{mn}} + N^{lin}_{(2)} \frac{\partial^2 P(\sigma_{ij},t)}{\partial \sigma_{mn}\sigma_{ab}} \tag{64}$$

where:

$$N^{lin}_{(1)} = \sum_{s=0}^{M} r^{s^{(k)}}_{mnab} \sum_{i=0}^{P} \langle \Phi_i \Psi_s \rangle \frac{1}{2\Delta t} \tag{65}$$
$$\sum_{j=1}^{N} \left[N_{j,b}(\mathbf{x}) \, \Delta d^{k-1}_{ija} + N_{j,a}(\mathbf{x}) \, \Delta d^{k-1}_{ijb} \right]$$

$$N^{lin}_{(2)}\left(r^k_s, \mathbf{x}\right) = t \sum_{s=0}^{M} \left(r^{s^{(k)}}_{mnab} \right)^2 \tag{66}$$
$$\sum_{i=0}^{P} \mathrm{Var}\left[\Phi_i \Psi_s\right] \frac{1}{4\Delta t^2} \left[N_{j,b}(\mathbf{x}) \, \Delta d^{k-1}_{ija} + N_{j,a}(\mathbf{x}) \, \Delta d^{k-1}_{ijb} \right]^2 .$$